Enabling Self Organisation for Future Cellular Networks

Iman Akbari

Submitted for the Degree of
Doctor of Philosophy

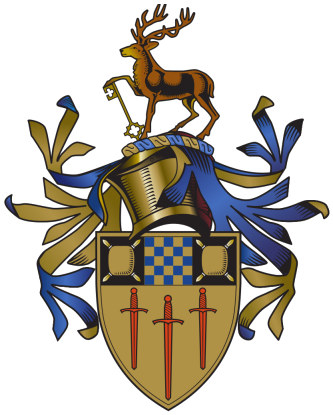

Institute for Communications Systems
University of Surrey

OCTOBER 2018

Abstract

The rapid growth in mobile communications due to the exponential demand for wireless access is causing the distribution and maintenance of cellular networks to become more complex, expensive and time consuming. Lately, extensive research and standardisation work has been focused on the novel paradigm of self-organising network (SON). SON is an automated technology that allows the planning, deployment, operation, optimisation and healing of the network to become faster and easier by reducing the human involvement in network operational tasks, while optimising the network coverage, capacity and quality of service. However, these SON autonomous features cannot be achieved with the current drive test coverage assessment approach due to its lack of automaticity which results in huge delays and cost. Minimization of drive test (MDT) has recently been standardized by 3GPP as a key self-organising network (SON) feature. MDT allows coverage to be estimated at the base station using user equipment (UE) measurement reports with the objective to eliminate the need for drive tests. However, most MDT based coverage estimation methods recently proposed in literature assume that UE position is known at the base station with 100% accuracy, an assumption that does not hold in reality. In this work, we develop a novel and accurate analytical model that allows the quantification of error in MDT based autonomous coverage estimation (ACE) as a function of error in UE as well as base station (user deployed cell) positioning. We first consider a circular cell with an omnidirectional antenna and then we use a three-sectored cell and see how the system is going to be affected by the UE and the base station (user deployed cell) geographical location information errors. Our model also allows characterization of error in ACE as function of standard deviation of shadowing in addition to the path-loss.

Acknowledgements

I would like to give my sincerest gratitude to my supervisors, Prof. M.A. Imran and Prof. R. Tafazolli, for the guidance, encouragement and support that they gave me throughout my research. Their enthusiasm and inspirational comments have ensured the success of this work.

I would also like to thank Dr. O. Onireti for all his help and valuable comments during the course of my PhD. In addition, I would like to thank all of those who supported me in any respect during this research.

Finally, I would like to thank my family for the love and support they have given me. Without them this journey would have not been possible.

Table of Contents

List of Figures

List of Tables

Glossary of Terms

3D	3-Dimentional
3GPP	3rd Generation Partnership Project
ACE	Autonomous Coverage Estimation
A-GPS	Assisted Global Positioning System
BS	Base Station
BSN	Body Sensor Network
CAPEX	Capital Expenditure
CCO	Coverage Capacity Estimation
CRS	Cell Specific Reference Signal
eLA	Enhanced Local Area
FDD	Frequency Division Duplex
GNSS	Global Navigation Satellite System
GPS	Global Positioning System
HetNet	Heterogeneous Network
ICIC	Intercell Interference Control
k-NNAD	k-Nearest Neighbour Anomaly Detector
KPI	Key Performance Indicator

LTE	Long Term Evolution
LTE-A	Long Term Evolution Advanced
MDT	Minimisation of Drive Tests
MRO	Mobility Robustness Optimisation
NCT	New Carrier Type
NGMN	Next Generation Mobile Networks
NMS	Network Management System
OMC	Operation and Maintenance Centre
OPEX	Operating Expenditure
OTDOA	Observed Time Difference of Arrival
QoS	Quality of Service
RACH	Random Access Channel
RAT	Radio Access Technologies
RAN	Radio Access Networks
RET	Remote Electric Tilt
RF	Radio Frequency
RRC	Radio Resource Control
RSRP	Reference Signal Received Power
RSRQ	Reference Signal Received Quality

RSS	Received Signal Strength
SINR	Signal Interference plus Noise Ratio
SO	Self-Organisation
SON	Self-Organising Networks
TCE	Trace Collector Entity
TXP	Throughput Power
UE	User Equipment
UMTS	Universal Mobile Telecommunications System
WLAN	Wireless Local Area Network

CHAPTER 1

1 Introduction

1.1 Context and Background

Every day more and more people are using their mobile devices to access the internet and the demand for wireless access is increasing exponentially which results in a rapid growth in mobile communications. The amount of IP data handled by wireless networks has increased significantly, and with this rate the amount will have increased 127-fold from 2005 to 2021. In 2016, global IP traffic was 1.2 ZB (ZB; 1000 Exabytes) per year and with this rate it will reach 3.3 ZB by 2021 with a compound annual growth rate of 24 percent from 2016 to 2021 [1] [2].

Consequently, the rapid growth is causing the distribution and maintenance of cellular networks to become more and more complex, expensive, and time consuming. Hence, there is an urgent need for a new functionality in cellular networks which would cope with this increased complexity, while reducing the cost and maintenance time.

Self-organisation (SO) is an adaptive functionality where the network can detect changes and based on these detected changes, makes intelligent decisions to maximise or minimise the effects of the changes [3]. Self-organisation is effectively the only feasible way of achieving optimal performance in future wireless cellular networks in a cost-effective manner [4]. Hence, standardisation bodies for long term evolution (LTE) and LTE advance (LTE-A) have

identified SO as not just an optional feature but an inevitable necessity in the future wireless systems [5].

Lately, extensive research and standardisation work has been focused on the novel paradigm of self-organising network (SON). SON aims at reducing the capital and operational expenditures (CAPEX & OPEX) significantly by reducing human involvement in network operational tasks, while optimising the networks coverage, capacity and quality of service [6]. In general, SON concept involves the integration of self-configuration, self-optimisation and self-healing functionalities into an automated process requiring minimal manual intervention [4] [6] [7]. SON is an automated technology that allows the planning, deployment, operation, optimisation and healing of the network to become faster and easier [8] [9]. However, these autonomous features cannot be achieved with the current drive test based coverage assessment approach, as it lacks automaticity and therefore results in huge delay and cost.

In legacy, cellular network cell outages are generally detected through, field drive tests, hardware or software failure alarms at the operation and maintenance centre (OMC), and complaints raised by the costumers. There are a few issues with these methods, firstly, these methods are manual and suffer from delays, also, the reliability of these methods is limited due to the human error factor in addition to the low spatiotemporal granularity of the reports and alarms available at OMC or measurements gathered through drive tests. On the other hand, in wake of 5G, cell densification is emerging as a dominant strategy for increasing cellular system capacity and quality of service [10]. With the increase in the cell density, the rate of cell outage is also bound to increase; hence, the manual cell outage detection methods cannot cope with the complexity and the expected rate of the cell outage in emerging ultra-dense networks, in a reliable and cost effective manner.

To overcome this challenge, 3GPP has standardized a SON use case, called minimization of drive test (MDT) [11], [12]. Hapsari et al. [11] describes in detail the solution adopted in 3GPP MDT whilst Baumann et al. [12] demonstrates that MDT can reduce drive tests. With MDT standardized, base stations will have access to the user equipment (UE) reported measurements that will consist of reference signal received power (RSRP) of the serving and neighbouring cells among other measurement reports. These measurements are called MDT measurements. Using MDT measurements level of coverage in an area of interest can be estimated without conducting expensive and time consuming drive tests or waiting for customer complaints. Cell

outages can thus be detected by applying data analytics and machine learning techniques of various types [13] [14] on the MDT reports.

However, most of these recently proposed methods that estimate coverage using MDT with different algorithms e.g., grey prediction, k-nearest neighbour anomaly detector (k-NNAD) [13] are facing a common challenge. These methods assume that UE position is accurately known at the base station. This assumption does not reflect the reality as even the most accurate UE positioning methods have a non-zero error range [15], [16].

Location information can be obtained by using positioning techniques, such as observed time difference of arrival (OTDOA) or assisted global positioning system (A-GPS) [15], [16]. For indoor environments, position estimation techniques based on WLAN, radio frequency identification (RFID) and ultrasonic have been proposed [17]− [18]. All these techniques are prone to errors. For example, the accuracy of A-GPS has been evaluated as 10 m, 10−20 m and 10−100 m for rural, suburban and urban environments, respectively. On the other hand, the average accuracy of indoor techniques is about 2m, however, they require installing specialised devices [17]− [18].

By exploiting the measurement reports gathered by the UEs and their location information, an autonomous coverage estimation (ACE) can be developed. In such a system, UEs measurement report such as received signal strength (RSS) are tagged with their geographical location information, which are obtained from the position estimation techniques, and sent to their serving base station. The serving base station after retrieving the measurements, further appends its geographical location information and forwards them to a trace collection entity (TCE), which then generates the autonomous coverage map. Since the position estimation techniques are prone to errors, the measurement reports may be tagged to a wrong location.

Enabling self-organisation is a key as we try to implement self-organisation in future networks by decreasing the amount of human intervention gradually to eventually reach zero intervention in deploying, optimising and managing future cellular networks. The main self-organisation enablers would be the seamless algorithms for autonomous coverage estimation, service estimation, cell boundary estimation, independent energy consumption and quality of service estimation. These estimation algorithms will provide the necessary data to help towards the full self-organisation and eliminating the need for human intervention in future networks.

The aim of the project is to perform self-organising coverage estimation for 5G cellular networks in an energy efficient manner. To do so, it's considered having a heterogeneous networks (HetNet) and splitting the C-plane and the U-plane. Also, phantom cells are used which are different to conventional "cells". So, the signalling and the data are split in which the signalling part is done by the macro base station and the phantom cells (data access points) deal with high capacity data transfers **FIGURE 1.1**.

The aim is that the base station by detecting the exact position of the users will decide how many small cells are required to be activated to cover all the users and then giving orders to the small cells to tilt their antennas in order to increase or decrease their coverage area to cover all the users. However, no matter what method it's used the position estimation of the users is not 100% accurate. This results in calculating the effects of inaccurate user position estimation and observing how this will affect the self-organising coverage estimation. Also, due to the fact that in future networks there are user deployed cells, hence the position estimation needs to be considered for the user deployed cells as well. This results in the need for calculating the effects of inaccurate position estimation for the user deployed cells in addition to the user position estimation error.

In addition, as green communication is becoming more important and more of a necessity for future networks. Hence, the aim is to achieve all these in an energy efficient manner. Through multi-cell cooperation, the number of active base stations can be decreased.

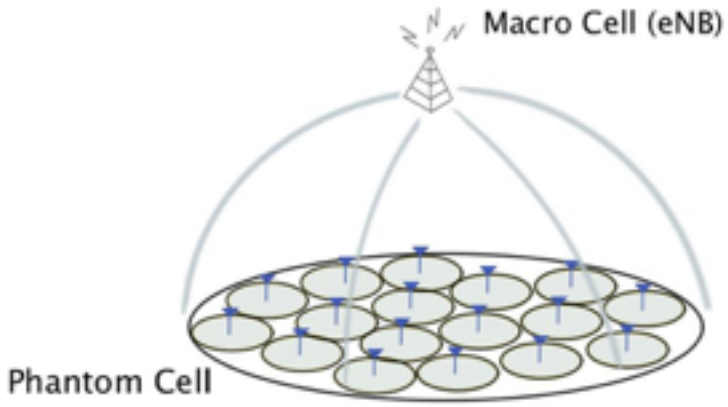

FIGURE 1.1: Umbrella Cell

1.2 Main Contributions and Achievements

Using MDT measurements level of coverage in an area of interest can be estimated without conducting expensive and time consuming drive tests or waiting for customer complaints. Cell outages can thus be detected by applying data analytics and machine learning techniques of various types on the MDT reports. However, all the methods assume that UE position is accurately known at the BS. This assumption does not reflect the reality as even the most accurate UE positioning methods have non-zero error range.

In this work, we address this challenge by analysing and quantifying the error in coverage estimation caused by the error in UE positioning. We investigate the impact of inaccurate position estimation on the ACE scheme by deriving its cell coverage probability over the area of interest where the data are gathered from.

We then extend the work by incorporating the impact base station position inaccuracy into the quantification of error in coverage estimation when the shadowing is considered in addition to the case with path loss only channel model. Significance of this work lies in the fact that results obtained can be used to calibrate the estimated coverage through MDT, for given values of standard deviation of shadowing and UE and base station positioning error range, in area under consideration.

Furthermore, we considered a three-sectored cell instead of the omnidirectional cell and investigated the impact of inaccurate UE and base station geographical position estimations on the sectors and how they will cause the UEs to be assigned to the wrong sector.

- A detailed ACE scheme is derived.
- The impact of UE position estimation on the ACE scheme is Investigated and shown.
- The base station (user deployed cell) positioning error is then added to the problem and the impact of it is investigated and shown.
- These errors are investigated for both cases of when shadowing is considered in addition to when the path loss only channel model is considered.

- At first an omnidirectional antenna is considered and then a 3-sector directional antenna is replaced.
- The impact of the UE and base station positioning errors are investigated on the 3-sector directional antenna.

1.2.1 List of Publications

During this PhD, the following publications have been produced:

Journal Papers:

- I. Akbari, O. Onireti, A. Imran, M.A. Imran, and R. Tafazolli, "How Reliable is MDT-Based Autonomous Coverage Estimation in the Presence of User and BS Positioning Error?," *IEEE Wireless Communications Letters*, vol. 5, no. 2, pp. 196-199, 2016.

Conference Papers:

- I. Akbari, O. Onireti, M.A. Imran, A. Imran, and R. Tafazolli, "Effect of Inaccurate Position Estimation on Self-Organising Coverage Estimation in Cellular Networks," *20th European Wireless Conference. EW2014*, pp. 1-5, Spain, Barcelona, 2014.
- I. Akbari, O. Onireti, A. Imran, M.A. Imran, and R. Tafazolli, "Impact of Inaccurate User and Base Station Positioning on Autonomous Coverage Estimation," *in proc. IEEE 20th International Workshop on Computer Aided Modelling and Design of Communication Links and Networks. CAMAD2015*, pp. 114-118, UK, Surrey, 2015.

1.3 Structure of Thesis

The remainder of this thesis is organised as follows:

Chapter 2: "Background and Literature Survey"

This chapter reviews the state of the art on self-organisation, capacity coverage estimation and minimisation of drive tests for future cellular networks. More precisely, in the first step, the concept of heterogeneous networks and phantom cells are reviewed. This is followed by a thorough review of self-organising networks, which involves self-configuration, self-optimisation and self-healing aspects. Next, the coverage capacity optimisation is reviewed with the inclusion of antenna parameters (antenna tilting and antenna pattern). This is followed by the conflicts avoidance in self organising networks which brings the essential need for coordination among self-organising functions. This is then followed by a detailed review of the drive test approaches. And finally, a thorough review of the position estimation is given.

Chapter 3: "Preliminary Investigations – Only Considering User Uncertainty"

This chapter provides the preliminary investigations on enabling SON. The impact of user geographical positioning error (GPS error) on the cell coverage is investigated. A single cell scenario is considered in which the cell coverage probability estimation for both the path-loss only channel model and when shadowing is added is derived. Some of the results in this chapter have been published in [19].

Chapter 4: "Autonomous Coverage Estimation – Considering Base Station and User Errors"

In this chapter, the effect of error in the user and base station geographical location information on the cell coverage estimation is investigated. An autonomous coverage estimation (ACE) schemes is introduced that exploits the measurement reports gathered by the UEs. The error in coverage estimation due to such autonomous scheme is evaluated by assessing the reliability of radio frequency (RF) coverage on the measurement based on the fundamental metric of cell coverage probability. This has been done for a single cell scenario and for both path-loss only channel model and the shadowing model. The results from this chapter have been published in [20] and [21].

Chapter 5: "Sectored Cell ACE"

In this chapter, the effect of error in the user and base station geographical location information on the cell coverage estimation is investigated, this is done whilst considering a three-sectored cell. An ACE scheme is introduced that exploits the measurement reports gathered by the UEs. The error in coverage estimation due to such autonomous scheme is evaluated and the effect of using a three-sectored cell instead of an omnidirectional antenna is investigated. This has been done for a single cell scenario.

Chapter 6: "Conclusion and Future Work"

In this chapter, a conclusive summary of the findings obtained by the work presented in the previous chapters is provided. Also, future research paths are proposed as a future work extension to continue the work presented in this thesis.

CHAPTER 2

2 Background and Literature Survey

This chapter reviews the state of the art on self-organisation, capacity coverage estimation and minimisation of drive tests for future cellular networks.

More precisely, in the first step, the concept of heterogeneous networks and phantom cells are reviewed. This is followed by a thorough review of self-organising networks, which involves self-configuration, self-optimisation and self-healing aspects.

Next, the coverage capacity optimisation is reviewed with the inclusion of antenna parameters (antenna tilting and antenna pattern).

This is followed by the conflicts avoidance in self organising networks which brings the essential need for coordination among self-organising functions.

This is then followed by a detailed review of the drive test approaches. And finally, a thorough review of the position estimation is given.

2.1 Heterogeneous Networks (HetNet)

Traditional wireless networks are optimised for homogeneous traffic. However, with the remarkable growth in cellular traffic, these traditional wireless networks face unprecedented

challenges to meet the demand in a cost-effective manner. Recently, the Third-Generation Partnership Project (3GPP) LTE-A has started to investigate heterogeneous networks (HetNet) deployments as an effective way to improve capacity as well as effectively enhance network coverage.

Unlike the traditional heterogeneous networks that deal with interworking of wireless local area networks and cellular networks, a HetNet is a network containing nodes with different characteristics such a radio frequency (RF) coverage area, radio access technologies and transmission power. In this system, the low power femto nodes and the high-power macro nodes can be maintained by the same service provider and they can share the same frequency band that the operator provides. So, to ensure the coverage of low power nodes, a joint resource/ interference management needs to be provided [22].

Although heterogeneous networks are envisioned to support the increasing data traffic demand and meet the requirements imposed for mobile networks, they also lead to new technical challenges. To successfully operate HetNets, radio resource allocator, control and management along with radio access and networking technologies are crucial.

In order to cope with the wireless traffic demand explosion, operators are underlying their microcellular networks with lower power base stations in a more dense manner buy using HetNets, or ultra-dense small cell networks.

Deployment of HetNets, require several challenges in terms of backhauling, capacity provision and dynamics in continuum fluctuating traffic load. This is where SON comes in as it has been defined to overcome these challenges [23].

As shows in FIGURE 2.1, heterogeneous cellular networks that consist of Macro and small cells can offer significant capacity gain by utilising the resources of the small cells. But to achieve this, the interference between the small cells and the macro cells must be carefully managed.

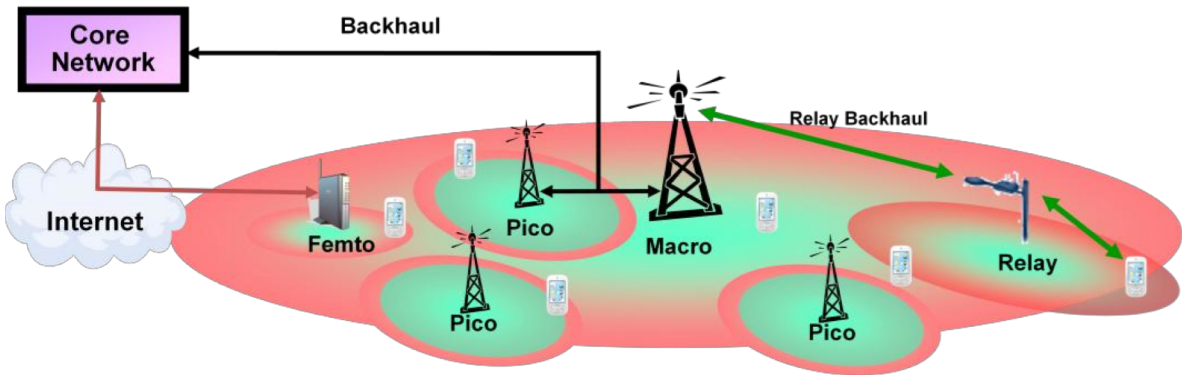

FIGURE 2.1: Heterogeneous Networks [24]

Noh et al. [25] proposes an uplink intercell interference control (ICIC) scheme which is a combination of the ICIC approach for the handover based and rate-split based interference controls.

It shows that the ICIC scheme works in distributed manner with low-complexity due to its controlled resource allocation so that it can be applied to self-organising network as well as heterogeneous networks.

Future cellular networks face a great challenge to meet the overwhelming demand for network capacity. Also, the increasing demand for higher data rates is leading to a rapid growth in power consumption and operating costs of cellular networks. One potential solution is to address these issues by overlaying small cell networks with macro cell networks to provide higher network capacity and better coverage.

However, such multi-tier network will raise issues regarding its energy efficiency implications due to the dense and random deployment of small cells.

Another technique to improve the energy efficiency in cellular networks is by introducing active/sleep moves in macro cell base stations.

Soh et al. [26] investigates the design and the associated trade-offs of energy efficient cellular networks through the employment of base station sleep mode strategies in addition to small cells. It derives the success probability and energy efficiency in homogeneous macro cell and

heterogeneous K-tier wireless networks for different sleeping policies using a stochastic geometry based model.

Karvounas et al. [27] considers a coverage and capacity optimisation problem in heterogeneous networks, where small cells are deployed within the area of macro base station. In order to maximise the users throughput without causing any interference to the other users, the small cells are configured to the optimal power level. At the same time, the redundant small cells are switched off to reduce the networks energy consumption.

2.1.1 Phantom Cell Concept

Over the last few years with the increased usage of smartphones and tablet devices, there has been a remarkable growth in cellular traffic. If this growth continues with this rate, current cellular capacity will not be able to support the future demand [28]. The current network deployment contains several capacity solutions for indoor environments such as Wi-Fi and femtocells. However, for high traffic outdoor environments, there is a lack of capacity solutions especially for the ones that can support good mobility and connectivity.

By using HetNet, significant capacity enhancements can be achieved. This is done by densely deploying various types of small cells in addition to the conventional macro cells. However, dense deployment of small cells in a co-channel deployment can result in interference between the small cells and the macro cells. As the macro cells provide the fundamental network coverage, hence, operators won't deploy small cell solutions if there's a chance that they would impact the key performance indicators of macro cell. Therefore, the phantom cell concept is introduced which is based on macro-assisted small cells. This concept is introduced as a capacity solution that offers good mobility support whilst capitalising on the excising Long Term Evolution (LTE) network [29].

In the phantom cell concept, the C-plane/U-plane are split (FIGURE 2.2). In this configuration, the C-plane must be supported by a continuous and more reliable coverage layer at lower frequency band while the U-plane can be provided by high capacity smaller cells. As it's shown in FIGURE 2.2, the C-plane of User Equipment (UE) in small cells is provided by macro cells in a lower frequency band to maintain good connectivity and mobility, while for the UE in

macro cells both the C-plane and U- plane are provided by the serving macro cell in the same way as in the conventional systems. On the other hand, the U-plane of the UE in small cells is provided by small cells in a higher frequency band. This is done so to boost the user data rate.

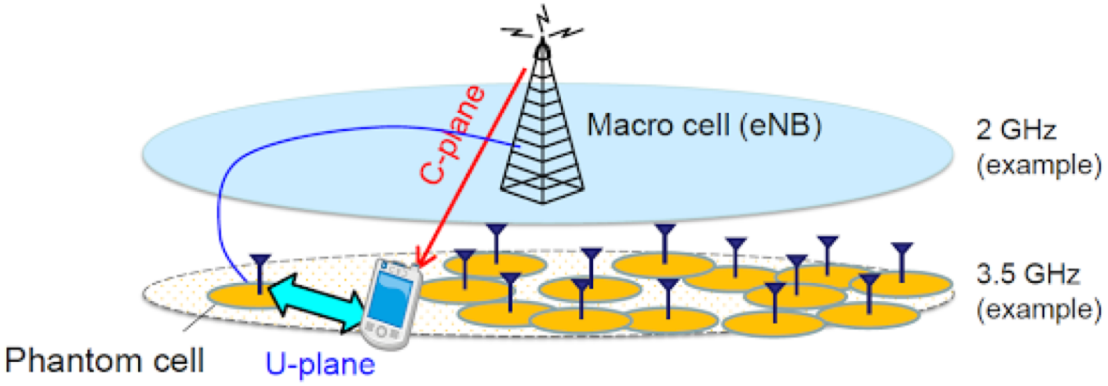

FIGURE 2.2: Phantom cell

These small cells (phantom cells) are not conventional "cells" because they are not configured with the cell specific signal and channels such as primary/secondary synchronisation signals and cell-specific reference signals (CRS). These cells visibility to the UE relies on the macro cell signalling. These macro-assisted small cells are called phantom cells dues to the fact that they are intended to transmit UE-specific signals only, and the radio resource control (RRC) connection procedures between the UE and the phantom cells are managed by macro cells.

There are a lot of benefits that come with the phantom cell concept. One of the benefits is that, network operators can maintain basic mobility and connectivity performance whilst they deploy only a small number go high frequency band cells. In addition to this, the phantom cell provides benefits such as energy saving efficiency, lower interference and so higher spectral efficiency by using the new carrier type (NCT) which contains reduced (or no) legacy cell specify signals.

At the moment, the 3GPP is standardising enhanced local area (eLA) small-cell heterogeneous architecture for inclusion in Long term evolution (LTE) release 12 as a solution offering high data rate to UEs along with high system capacity through spatial reuse of the spectrum.

Energy efficiency is becoming an important factor in evaluating the next generation of small cell networks.

Mukherjee et al. [30] focuses on phantom cell architecture which is a eLA architecture. It uses the results from stochastic geometry to compare the energy efficiency of the phantom cell architecture versus the baseline small cell network, defined as conventional frequency division duplex (FDD) LTE pico-cell deployment that uses the same spectrum as the underlying macro cellular network.

The 3GPP standardisation body has initiated studies on LTE rel. 12 to cope with the expected growth in mobile data traffic by 2020 [31].

Cellular networks are usually modelled by placing the base station on a grid, with mobile users either randomly scattered or placed deterministically. These models suffer from being both highly idealised and not very tractable, so complex system-level simulations are used to evaluate coverage/outage probability and rate.

Andrews et al. [32] develops new general models for the multi-cell signal to interference plus noise ratio (SNIR) using stochastic geometry. The presented framework is significantly more tractable than the traditional grid-based models, and appears to track a real deployment as accurately as the traditional grid model. In addition to being more tractable, the presented models may better capture the increasingly opportunistic and dense placement of base stations in future networks.

2.2 Self-Organising Networks (SON)

Self-Organisation (SO) has been defined in various fields including biology and computer science. In general, self-organisation is the spontaneous often seemingly purposeful formation of spatial, temporal, spatiotemporal structures or functions in systems composed of few or many components.

Self-Organisation can be seen in both animate and inanimate worlds. In animate world, objects grow, change in form and function without being created by humans. Even human brain may be considered as a self-organising system. On the other hand, in the inanimate world, planetary systems and the galaxies are examples of as self-organisation [33].
In definition, SO is referred to as an intelligent system that would learn from the environment and adapt to statistical variations in input stimuli to achieve highly reliable communications whenever and wherever needed [34]. In networks, the term self-organising networks is generally taken to mean a cellular network in which the configuration, the operation and the optimisation tasks are largely automated [35].

The increase in user applications requires an increase in the capacity of cellular systems. Also with the growth of technology, users are expecting to receive better quality of service (QoS). As a result, the operators are looking for ways to increase the capacity and the quality of service. Since higher capacity and QoS will result in a higher capital expenditure (CAPEX) and operating expenditure (OPEX), and since users may be reluctant to pay proportionally higher bills for improved services; the operators aim to reduce and minimise CAPEX and OPEX whilst enabling a gratifying user experience even under adverse conditions such as congested traffic [4]. Also with radio networks like the ones used for LTE and other cellular technologies becoming more complex, network planning needs to be made easier. As a result, the concept of self-organising networks is growing in interest and use. The increasing in data usage has resulted in more dense and complicated networks, this in turn has caused the network planning and maintenance to be more complicated than in the early days. Most of this is due to the introduction of LTE in which ensures the total minimum capacity has been met by increasing the node density with low power nodes such as micro cells, femtocells and relay points [36].

Self-organisation has been investigated in different types of communication networks. In context of wireless cellular networks however, self-organisation is a relatively new yet rapidly growing area when compared to ad hoc networks or wireless sensor networks.

SON has been introduced with the main following aims:

1. Reducing OPEX by decreasing the level of human intervention in the design, build and operation of the network.
2. Reducing CAPEX by making use of the available resources and optimising them.
3. Protecting revenue for the operators by reducing the number of human errors. [36]

Using SO-enabling systems [37], small cells can sense, learn from their environment, and autonomously tune their transmission strategies toward an optimal performance. Moreover, many advantages can be obtained with SO technologies, such as minimising human intervention in networking processes and allowing operators to streamline their operations [38].

SON solutions can be divided into three main categories, self-configuration, self-optimisation and self-healing. The SON architecture can be centralised, distributed or a hybrid solution [39].

2.2.1 Self-Configuration

Configuration of base stations/eNodeBs, relay stations and femtocell is required during deployment, extension and upgrade of network terminals. It may also be needed when there's a change in the system, for example a failure of a node. In future systems, the conventional process of manual configuration needs to be replaced by self-configuration. In self configuration, the aim is for the base stations to become essentially plug and play items. So, through SON new cell sites can be added to the network using plug and play and they should need as little manual intervention in configuration as possible. This will reduce the level of installer input so the skill level of the installer can also be reduced, therefore, saving cost while improving the reliability of the system by the reduction of installer input. Accordingly, this is a major element within SON [4] [36].

As self-configuration is of use for this work, we'll focus more on it in the next section.

2.2.2 Self-Optimisation

After the initial self-configuration phase where the system has been set up, it is necessary to optimise the operational characteristics to best meet the needs of the overall network and continuously optimise the system parameters to ensure performance of the system is efficient if all its optimisations are to be maintained. This is achieved by self-optimisation routines within the overall SON. In general, optimisation is required to ensure that when a cell has been installed, it operates at its best level of efficiency. Self-optimisation network techniques can analyse the performance of the network and change it to best meet the needs of the operator and the users [4] [36].

Self-optimisation is important for HetNet implementations for achieving automatic optimisation decisions and procedure executions [37] [40].

Self-optimisation functionality monitors and analyses performance management data, and when necessary, automatically triggers optimisation action on the affected network node(s). This significantly reduces manual interventions and replaces them with automatically triggered re-optimisations, re-configurations, or software reloads/upgrades thereby helping to reduce operating expense [41].

SON self-optimisation also includes:

- Load balancing
- Handover parameter optimisation
- Interference control
- Capacity and coverage optimisation
- Random access channel (RACH) optimisation

As capacity and coverage optimisation is of use for this work, we'll focus more on it in the next section.

2.2.3 Self-Healing

Most system will develop faults from time to time and this is the same in wireless cellular systems. This can be due to component malfunction or natural disaster. The faults caused can cause major inconvenience of the users, however, it is often possible for the network to change its characteristics to mask the effects of the fault temporarily while the repairs are being effected on the cellular networks. To do so the boundaries of the adjacent cells can be increased by increasing the power levels and changing antenna elevation levels, etc. [4].

The self-healing aspect of SON is an increasingly important element of the overall cellular networks. It involves remote detection, diagnostic and triggering compensation or recovery action to mitigate the effect of the faults in the network equipment's [36] [42].

According to architectural categorisation, the SON approach can be designed by using the following different classes depending on the location of optimisation algorithms: centralised SON, distributed SON, localised SON and hybrid SON [43]. A hybrid SON is usually required in practice. In centralised SON, a large number of cells are involved in the optimisation and due to the long-term statistics being processed, slower parameter update rates are faced. In centralised solutions, the SON functionality is located at a high level in the architecture such as network management system (NMS). The use cases in centralised SON are such that they require many cells to be treated simultaneously, e.g., if the antenna tilt of a base station is changed; it must be considered in the neighbouring cells due to the changed interference situation [44]. Distributed SON is applied in the optimisation processes that involve only a few cells (e.g., two cells). In distributed SON the optimisation algorithm are executed in the base station. Localised SON is applied to the single cell processes. These don't have significant impact on their neighbours [45].

Lateef et al. [46] presents a self-coordination framework which builds on the comprehensive identification and classification of potential conflicts that are possible among the major self-organising functions envisioned by the 3GPP so far.

The classification is achieved by analysing network topology mutation, temporal and spatial scopes, parametric dependencies, and logical relations that can affect the operation of self-

organising functions in reality. and it outlines a solution approach for a conflict free implementation of multiple self-organising functions in LTE/LTE-Advanced networks.

Diagnosis for configuration troubleshooting in femtocell networks is extremely important for end users and network operators. But because the small sized femtocells only serve several users, the historical data are insufficient. This makes traditional cellular troubleshooting solution which require a large amount of historical data not applicable.

Wang et al. [47] proposes a transfer learning framework for diagnosing femtocell configuration problems which is based on transfer learning technology to address the data scarcity to enhance the accuracy of the diagnosis model. To do so it extracts additional diagnosis knowledge by transferring data information from other femtocells. It's also shown that by doing extensive evaluations, this approach can achieve higher accuracy than traditional methods in self-organising femtocell network scenarios.

The general idea of a SON is to integrate network planning, configuration, and optimization into a unified automatic process requiring minimal manual intervention [37].

Parodi et al. [48] presented a general framework for self-configuration of future LTE networks that addresses the problems associated with autonomous deployment of a new site i.e. without the need for any human intervention. In future cellular networks, nodes should be able to self-configure all the initial parameters including IP addresses, neighbour lists and radio access parameters.

3GPP Releases 8 and 9 specify the most important SON related objectives, include interference control, coverage capacity optimisation (CCO), mobility load balancing, mobility robustness optimisation (MRO), and energy saving management for homogeneous topology [37] [49].

For this work we focus more on the CCO.

2.3 Coverage Capacity Optimisation (CCO)

The concept behind CCO is to adapt parameters such as antenna tilts and transmitter power levels to maximise coverage while optimising the capacity by insuring inter-cell interference levels are minimised. This can create some significant advantages that can be very time consuming and expensive to manage manually [50].

The objective of CCO is to provide optimal coverage and capacity for the radio network. This needs to be done whilst considering a trade-off between capacity and coverage.

Coverage optimisation is very important within cellular networks. It is important that in the network, the cells provide a complete coverage without having areas with no coverage at all. The coverage area of each cell is determined through multiple factors; position of antenna, transmission power and antenna tilt.

To reach the CCO targets, the following parameters may be optimised [51] [50]:

- **Downlink transmit power:** The transmitter power optimization is more challenging than optimising antenna parameters. There are issues with amplifier behaviour and issues with reciprocity with the handsets. It is possible to increase the transmitted power so that the handset receiver can receive the base station further away, but it may not be possible for the handset to increase its power sufficiently to match any improvements specially at the cell edge where it may already be operating close to its maximum level.
- **Antenna parameters (tilt and azimuth):** To achieve CCO using the adjustment of the antenna parameters, a remote electric tilt (RET) is required. The adjustments can be made either electrically or mechanically, however, sometimes both are needed for a wider range. The antenna tilt needs to be carefully adjusted to not produce coverage holes or increase the interference by tilting too much or too little. The antenna azimuth is the direction that the antenna is pointing (only for directional antennas, not omnidirectional antennas).

To optimize coverage within the network, since these can be executed remotely, usually a sequence of power and tilt adaptations is used. Then the situation is re-evaluated after each

change through the analysis of measurement reports. The results of these evaluations are used to determine whether additional adaptions are required or not [52].

The use case of CCO is to enable detection of following problems:

- Priority 1: coverage problems, e.g. coverage holes
- Priority 2: capacity problems

The work on the detection methods is to be coordinated with the progress of other SON functionalities, in particular, mobility robustness optimisation (MRO) and minimisation of drive tests (MDT) [49].

2.3.1 Antenna Tilting

Antenna tilt is one of the most important system parameters in coverage and capacity optimisation as tilt determines the service coverage boundary and level of inter-cell interference in the system [53].

There are two ways of tilting the vertical pattern of an antenna, mechanical tilting and electrical down-tilt [54].

Mechanical tilting

The easiest way of beam tilting is to mechanically tilt the entire sector antenna using brackets. But this is a less favourable way of beam tilting as it has a significant downside. This technique does not reduce the converge consistently across the horizon over whole sector. Mechanical tilting reduces coverage more in the bore sight - the direction along which the gain is maximum is called the antenna bore sight for a directional antenna [55]- direction and less at other angles away from the bore sight. This results in an inconsistent decrease in the cell coverage area which is referred to as pattern blooming.

Electrical down-tilt

Normally to reduce the network inefficiencies, the acceptable amount of pattern blooming should not exceed 10% of the antennas azimuth beam width. Higher levels of pattern blooming will generate interference levels that can cause network inefficiencies and diminish the quality of service.

A more preferred method for tilting the vertical pattern of a sector antenna is by using electric down-tilt. The way this technique works is that by using phase shifters, it manipulates the electric phase derived to each antenna element to achieve beam tilting. The antenna itself remains mounted upright and is not tilted (mechanically) while the RF signal shifts and the resulting elevation pattern is tilted consistently over the entire 360 degrees, reliably shrinking the coverage area. This method won't affect the amount of pattern blooming and pattern blooming won't increase regardless of the amount of electric down-tilt.

Another advantage of this method (electric down-titling) is that by connecting a motor to the phase shifter mechanism, the whole thing can be done remotely. This advantage is becoming more important by the increased use of the next generation air interface technologies such as LTE [54].

SON is linked closely to LTE. wherein the network re-optimises itself routinely based in demand levels. For the full SON concept implementation, flexible coverage adjustment techniques such as electric down-tilt are required.

Performance and efficiency of a cellular network antenna can be enhanced by properly adjusting the antenna tilt settings. Antenna tilt is one of the most important radio parameters that determine the service coverage boundary and level of intercell interference in cellular systems.

In addition, tilt tuning is an effective technique in radio network optimisation to affect a better load balance among cells for effective utilisation of spare radio resources. the variability of user traffic distribution makes it more challenging for operators to ensure the required service capacity and quality with acceptable capital and operational expenditures.

Kifle et al. [56] investigates the potential performance gains of tilt optimisation for differently placed user traffic concentrations. It shows using simulations that the users at traffic hot spot area suffering from resource sharing can achieve significant performance gains (resulting from

coverage change due to tilt adaptation leading to the signal to interference plus noise ration (SINR) improvement of hot spot areas) from traffic oriented tilt optimisation.

Popup traffic hotspots are a time persistent reason behind poor user experience in wireless cellular systems. The unpredictability of these hotspots makes them difficult to be designed out in the planning phases of the cellular system, hence, dynamic and adaptive solutions are required to deal with this.

Imran et al. [57] presents a novel solution to address the popup traffic hotspots issue by dynamically enhancing spectral efficiency in hotspot region through optimisation of system wide base station antenna tilts in distributed fashion. The solution provided, unlike most of the existing works, doesn't rely on load transferring to neighbour cells; rather it dynamically enhances the overall spectral efficiency and thus the capacity of the system by jointly optimising antenna tilts of multiple adjacent cells with respect to hotspot locations in those cells. A pre-determined set of neighbouring cells jointly optimise their tilts to focus their antenna gains at the centre of gravity e.g., hotspots in those cells.

2.3.2 Antenna Azimuth

Azimuth refers to the rotation of the whole antenna around a vertical axis. The antenna azimuth is the direction that the antenna is pointing (only for directional antennas, not omnidirectional antennas). The azimuth plane pattern is formed by slicing the 3D pattern through the horizontal plane (the x-y plane). This can be seen in FIGURE 2.3.

2.3.3 Antenna Pattern

Antenna pattern is the graphical representation of the radiation properties of the antenna as a function of space. In other words, the antenna’s pattern describes how the antenna radiates energy out into space (or how it receives it) [58].

The antenna pattern is three-dimensional. This is due to the fact that an antenna radiates energy in all directions. This 3D pattern is described with two planar pattern called the principal plane patterns. These principal plane patterns that are commonly referred to as the antenna patterns are shown in FIGURE 2.3 and FIGURE 2.4.

The terms azimuth plane pattern and elevation plane pattern are commonly used regarding antenna patterns. Azimuth and elevation are angles used to define the apparent position of an object in the sky [59]. The terms azimuth and elevation are normally referenced to the horizon and the vertical respectively whereas the azimuth angle is the compass bearing and the elevation angle is the altitude [60]. This is shown in FIGURE 2.3.

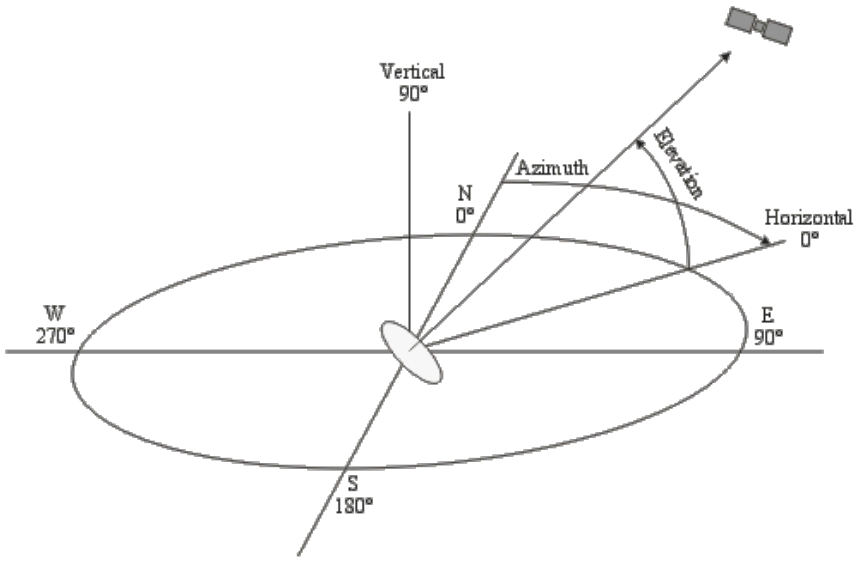

FIGURE 2.3: Graphical explanation of antenna azimuth and elevation [61]

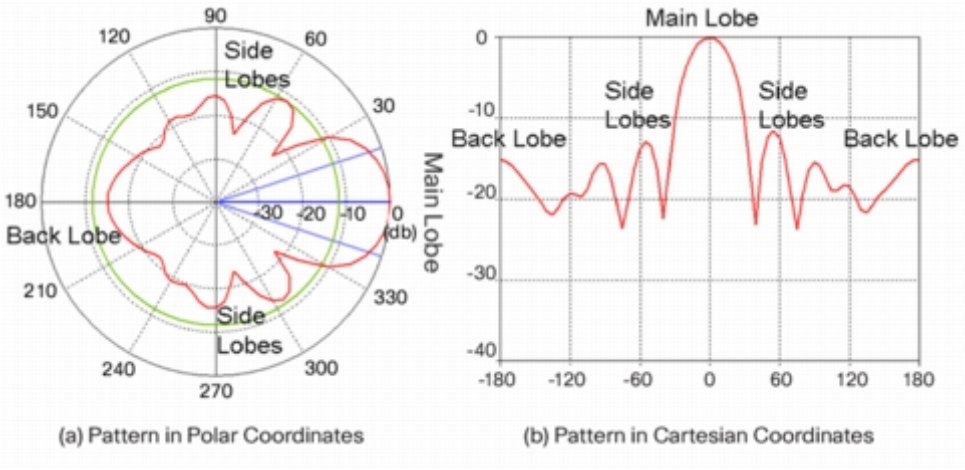

FIGURE 2.4: Radiation pattern in polar and Cartesian coordinates showing various types of lobes [58]

2.4 Conflict Avoidance

Self-organising functions may have complex relations and parameter/logical inter-dependencies which can induce conflicts among self-organising functions and eventually undermine the network operation. Therefore, to ensure the stable operation of wireless networks, in addition to avoiding objective/parameter conflicts, coordination among self-organising functions is essential.

It is vital to figure out the optimum way of designing self-optimisation algorithms in conjunction with self-coordination for efficient radio resource management and reduction of OPEX. If for example, the self-optimisation and the self-coordination are executed independently, this will cause the algorithm part of the self-optimisation function to be executed without the subsequent knowledge or rejection of the action requested by self-coordination function. This in turn may result in numerous self-optimisation algorithms to be executed without any performance gains [46].

In [62] the initial challenges of characteristics, parametric, and measurement conflicts when integrating SON functions into next generation wireless networks were described. However,

none of these works provide comprehensive identification, annotation, and classification of SON function conflicts.

Bandh et al. [63] presents an experimental system for SON function coordination based on flexible policy based decisions. Coverage and capacity optimisation (CCO) is presented as a use case to demonstrate successful coordination of multiple independent SON functions. CCO is performed through adaptations of throughput power (TXP) and antenna tilt (RET). Subsequent CCO(TXP) and CCO(RET) requests for changing the respective parameters need to be coordinated because they depend on the changes previously performed at a cell.

In [46] the authors have identified and annotated several possible conflicts among the range of self-organising functions anticipated to be implemented in LTE and LTE-Advanced. It has also presented a comprehensive taxonomy of these conflicts, which classifies them based on network topology mutation, key performance indicator (KPI), output parameters direction/magnitude, measurement and logical dependency conflicts. However, the resolution of SON conflicts requires a deeper analysis, modelling, and classification.

With the introduction of SON, there may be a risk for conflict and dependencies between SON functions, which may result in a suboptimal performance. Schmelz et al [64] concludes that, a SON Coordinator may be beneficial to prevent from network instabilities and/or to improve the performance; in case several conflicting SON functions are implemented in a network.

This deeper analysis, modelling, and classification can be seen in [65] where a comprehensive classification of SON function conflicts, which leads the way for designing suitable conflict resolution solutions among SON functions and implementing SON in real world is presented. The analytical model of these conflicts is presented using reference signal received power plot in multi-cell environments, which helps to dig into the complex relations among SON functions.

In [52], based on a detailed analysis of the requirements for the coordination, a policy-based approach to realise the coordination-related decision making based on the network configuration and SON function context is presented. Results for two use cases are presented to show the applicability of the developed approach to diverse SON use cases.

2.5 Drive Test Approaches

To provide a good network coverage and QoS, mobile communication networks are required to be monitored and optimised. The cellular network operators have the important task of drive testing to constantly assess the quality of their networks.

Drive tests are used to collect data from mobile networks and use these data for the configuration and maintenance of the networks. Conventional drive testing is a manual process in which the operator would be required to send engineers to the field to collect radio measurements in a hand-operated manner. In turn this helps them to discover network problems such as coverage holes in their networks and to be able to enhance the quality of their networks. However, such conventional drive tests consume significant time and human efforts to obtain and require a large OPEX while the collected measurements only cover a certain area of the network and can only give limited snap shots of the entire networks [62] [11].

These issues have been discussed by the operators in the Next Generation Mobile Networks (NGMN) alliance - a non-standardisation organisation- where the requirements for the automated drive tests and the recommendation solutions were delivered [66].

To reduce the effort and expense of drive tests, the 3GPP studied and specified solution in release 9 under the name “Minimisation of Drive Tests” (MDT) scoping two Radio Access Technologies (RATs), LTE and Universal Mobile Telecommunication Systems (UMTS). The main concept is to take advantage of UEs measurement capabilities to use each device which is logged in the network for collecting measurement data. The work was finalised as part of 3GPP release 10 specification [67] [11] [12].

In [67], the main use cases for MDT are defined by the 3GPP Technical Specification Group Radio Access Networks (RAN). They are; coverage optimisation, mobility optimisation, capacity optimisation, parametrisation for common channels and QoS verification.

With MDT, in addition to OPEX reduction, the data collected reflects the real-time network quality of where the users are actually located. This cannot be achieved by conventional drive tests and is an essential value of MDT. An operator, with the effective use of MDT, can potentially eliminate frequent needs for traditional drive tests and realise the real-time optimisation of networks [11].

Baumann et al. [12] talks about MDT and how it can reduce drive tests; especially for coverage, capacity and QoS. But there are still use cases where MDT cannot replace drive tests. For example, for a detailed detection of coverage holes or hidden neighbourhoods, a drive test is needed.

Johansson et al. [68] describes the MDT enhancements added in 3GPP release 11 specification in order to provide a more complete view of the network performance. These MDT enhancements, enable the operators to collect measurements indicating the users' real-life throughput and connectivity issues in addition to those indicating the network coverage conditions. This results in a wider application of use cases that allows network optimisation without dependence on conventional drive tests.

In [69], measurement reports from UEs are used for MDT. In this MDT system, UEs upload the measurement reports periodically or upon request and based on these measurement reports, the MDT system learns the knowledge about the communication environment.

A generic measurement architecture for automating the collection of UE radio measurements in order to minimise the need for manual drive tests in HetNet small cell networks is proposed in [70].

A user satisfaction classification for MDT QoS verification is proposed in [71]. It introduces a data mining framework which allows to distinguish between satisfied and unsatisfied users in LTE mobile networks on the basis of limited number of KPIs.

2.6 Position Estimation

Various location based services in wireless communication networks depend on mobile positioning. commercial examples range from low-accuracy method based on cell identification to high-accuracy methods combining wireless network information and satellite positioning. These methods are typically network centric, where the position is determined in the network and presented to the user via a specific service.

A position estimation method is demanded to provide location-based services such as navigation in recent years. Such services require the real-time position of the user. Global

positioning system (GPS) is one of the well-known position estimation methods. However, GPS cannot accurately determine the position in indoor environments.

For indoor environments, many position estimation methods using WLAN [72], RFID [73], ultrasonic [74] and etc. have been proposed. However, these methods require installing specialised devices to the environment [75].

Today, the global navigation satellite system (GNSS) is the most effective positioning technology in the outdoor open environments [76]. However, it has limitations such as poor performance in built-up areas and high power consumption. which has led to the development of positioning techniques that are based on the wireless networks. These technologies include a variety of angle of arrival, time of arrival and location fingerprinting techniques.

RF fingerprinting refers to a database correlation method where the position is estimated by comparing the radio measurements e.g., the RF fingerprint of the UE with the training fingerprint consist of received signal strength (RSS) radio measurement from several base stations that are used to provide a fingerprint of the radio conditions at a specific geographical location. normally this location is determined with an accurate positioning method (i.e. GNSS). hence, fingerprinting is a positioning method that make the most of the already existing infrastructures such as cellular networks [77] and WLANS.

Mondal et al. [78] estimates the position using the grid based radio frequency fingerprint position estimation. It proposes a novel technique to enhance the performance of this grid based RF fingerprint position estimation framework by introducing an overlapping grid layout to form training signatures and by estimating the location of the testing signature to be a weighted geometric centre of a set of nearest grid units. The enhancements can increase the number of training signatures that is required to be analysed for finding the nearest grid but the position accuracy is increased.

Kaneto et al. [75] proposes a method for estimating the user position in an indoor environment where the user is holding a microphone (phone). In this method, digital watermarking for audio signals is used. A model of the detection strengths is constructed and using the model the user position is estimated in real life. The estimation accuracy of the case has been evaluated for both static user and moving user. However, this method is dependent on the area of the environment and the number of loudspeakers.

Tsuji et al. [79] proposes a users' position and behaviour estimation method using sensors such as GPS device, an acceleration sensor and an ultrasonic sensor, to alert important information to the user at the right time. In the work the aim was not detecting the precise users' location but rather estimating the users rough position and rough behaviour (walking, running and etc.).

Hoseintabatabaei et al. [80]presents a novel approach for mobile phone centric observation of a user's facing direction, relying solely on built-in accelerometer and magnetometer. This approach achieves greater accuracy and independence by an automatic detection of the wearing position of the mobile device on the user's body and subsequent selection of an optimum strategy for estimating the user direction.

In order to observe a users' directionality, current approaches make use of, ambient sensors, body sensor networks (BSN) and localisation with wireless transceivers (e.g. GPS or Wi-Fi) or GPS sensors. Most of these have limitations to either the location or the duration of the observation. The limitations are either due to dependency of ambient sensors and wireless technologies on infrastructures deployed in an environment or the effect of the environment (e.g. indoor signal blockage or GPS) on the utilised techniques.

As the algorithm only relies on embedded accelerometer and magnetometer sensors of the mobile phone, it is not susceptible to shadowing effect as GPS.

Summary

In this chapter, the state of the art on self-organisation, capacity coverage estimation and minimisation of drive tests for future cellular networks is reviewed. More precisely, in the first step, the concept of heterogeneous networks and phantom cells are reviewed. This is followed by a thorough review of self-organising networks, which involves self-configuration, self-optimisation and self-healing aspects. Next, the coverage capacity optimisation is reviewed with the inclusion of antenna parameters (antenna tilting, azimuth and antenna pattern). This is followed by the conflicts avoidance in self organising networks which brings the essential need for coordination among self-organising functions. This is then followed by a detailed review of the drive test approaches. And finally, a thorough review of the position estimation is given.

CHAPTER 3

3 Coverage Estimation Considering User Position Uncertainty

In this chapter, the effect of inaccurate user position estimation (GPS error) on the cell coverage is investigated. A single cell scenario is considered in which the cell edge and coverage probabilities for both shadowing and non-shadowing cases are derived.

3.1 Technical Approach

We consider that, self-reports of measured received power at each reporting user-equipment are collected in a central location. All these measurements are tagged with the geo-location of the user (which is estimated by the user using some mechanism that is prone to error such as GPS). We aim investigating the impact of the position estimation error on the coverage estimation.

In the works that has been carried away for this research, in order to be able to investigate the cell and its surroundings easier, the cell has been assumed to be circular with a radius of ***R*** and is positioned at the coordinates ***(a, b)***.

Also, it has been assumed that the system (GPS) that is responsible for estimating the position of the user has a resultant error radius of ***r*** from the actual position of the user with coordinates

(c, d). Hence, this results in an imaginary circle with radius ***r*** being drawn around the actual position of the user in which the system may take any point in this imaginary circle as the estimated position. The cell and the way the user is positioned can be seen in FIGURE 3.1(a).

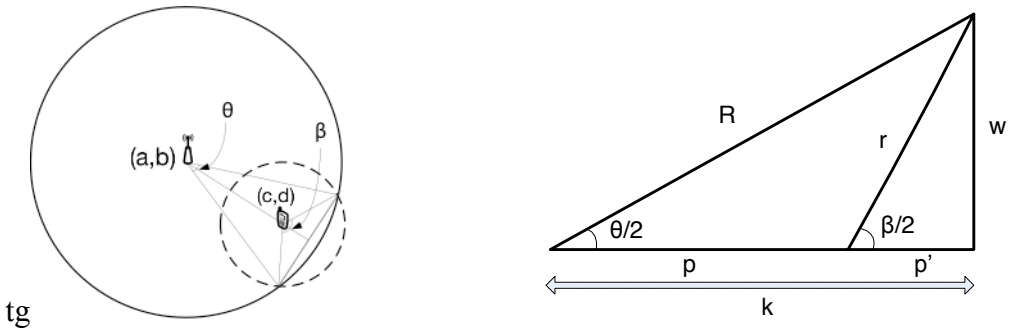

(a) Cell and user positioning

(b) Calculating the angle

FIGURE 3.1: (a) UE with reported position *o*, its actual position lies within the circular disc with radius *r* centred *o*. (b) shows the triangle created in (a).

To find the probability of inaccurate position estimation, the area of the imaginary circle that lies outside the cell needs to be calculated.

Area Calculation

The first step is to find the distance between the centre of the cell to the exact user position, as shown in (1):

$$p = \sqrt[2]{(c-a)^2 + (d-b)^2} \tag{1}$$

By drawing the radius of the cell perpendicular to the line connecting the intersecting points (between the cell and the imaginary circle around the user), a triangle will be produced as shown in FIGURE 3.1(b).

Using the produced triangle shown in FIGURE 3.1(b) and some trigonometry, the angles $\boldsymbol{\theta}$ and $\boldsymbol{\beta}$ can be calculated. The results are shown as followed in (2) and (3).

$$\theta = 2.\cos^{-1}\left[\frac{R^2 + p^2 - r^2}{2.p.R}\right] \tag{2}$$

$$\beta = 2.\cos^{-1}\left[\frac{R^2 - p^2 - r^2}{2.p.r}\right] \tag{3}$$

By taking and the cell sector and the line connecting the intersecting points (between the cell and the imaginary circle around the user), the area of the first segment shown in FIGURE 3.2(b) can be calculated using (4).

$$A_1 = (1/2).(\theta - \sin\theta).R^2 \tag{4}$$

Now by taking the sector in the imaginary circle around the user and the line connecting the intersecting points, the area of the second segment shown in FIGURE 3.2(a) is calculated and can be seen in (5).

$$A_2 = (1/2).(\beta - \sin\beta).r^2 \tag{5}$$

From (4) and (5), the area of the imaginary circle positioned outside of the cell (FIGURE 3.2(c)) can be calculated by subtracting the area of the first segment from the area of the second segment as shown in (6).

$$A = A_2 - A_1 = (1/2).\left[\left((\beta - \sin\beta).r^2\right) - \left((\theta - \sin\theta).R^2\right)\right] \tag{6}$$

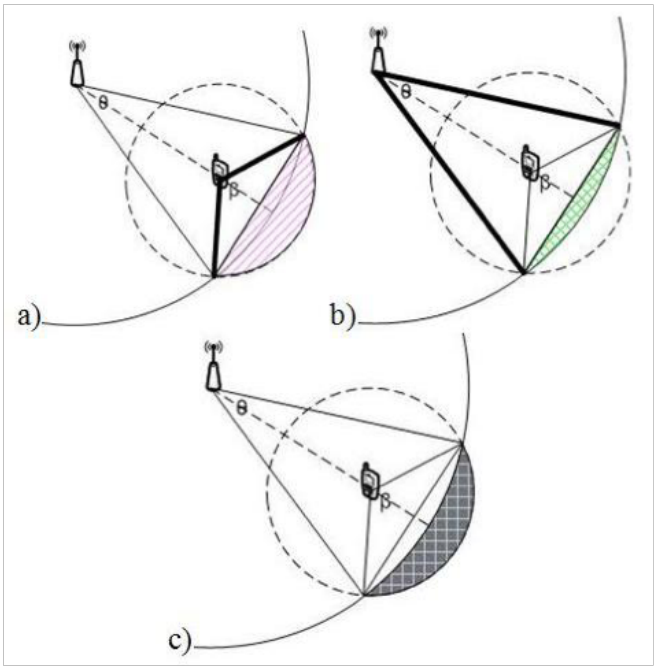

FIGURE 3.2: (a) Area of the first segment, (b) area of the second segment, and (c) area outside of the cell.

However, there is a special case where the area that lies outside of the cell can't be calculated using (6). This case happens when the user is positioned somehow that the line connecting the intersecting points is on the other side of the user (the user is closer to the edge of the cell). This can be seen in FIGURE 3.3(a). In this case, the angle passes the 180 degrees ($\boldsymbol{\pi}$) mark and is obtuse.

Similar to the previous section, the area of the first segment (FIGURE 3.3(b)) is calculated using (4). However in this case, the area found using (5), calculates the area of the shaded segment inside of the cell as shown in FIGURE 3.3(c).

Therefore, in order to calculate the area that lies outside of the cell, the area of the first segment is added to the area of the second segment and then subtracted from the whole area of the imaginary circle. This can be calculated using (7).

$$A = \pi.r^2 - (A_2 + A_1) = r^2.\left[\pi - \frac{(\beta - \sin\beta)}{2}\right] - \left[\frac{(\theta - \sin\theta).R^2}{2}\right] \quad (7)$$

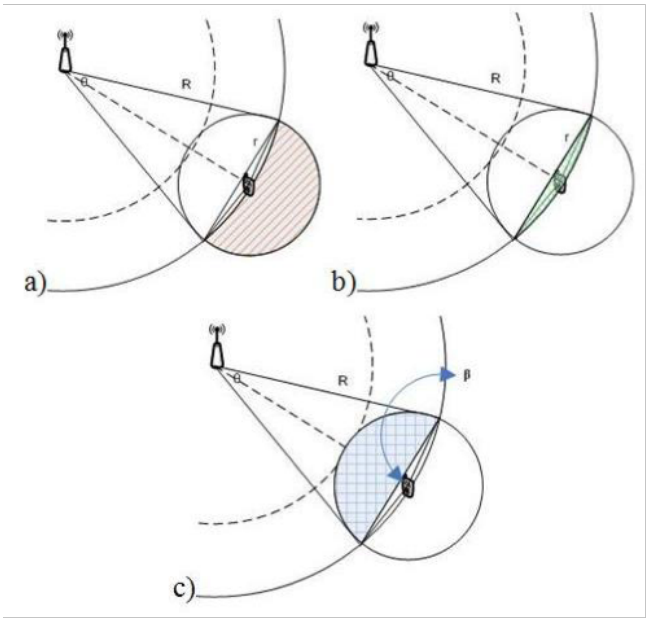

FIGURE 3.3: (a) Area of the first segment, (b) area of the second segment, and (c) area outside of the cell for the special case.

(6) and (7) can be simplifies into (8) as,

$$A = \begin{cases} A_2 - A_1, & if\ \beta < \pi \\ \pi.r^2 - (A_2 + A_1), & if\ \beta > \pi. \end{cases} \quad (8)$$

3.2 System Model and Performance Metrics

Two fundamental measures of reliability of RF coverage are utilised, i.e., cell edge reliability and cell coverage probability, to demonstrate the effect of inaccurate position estimation in self-organising cellular networks.

3.2.1 Propagation Model

The degradation of the signal quality is usually assumed to be due to three different causes: fast fading, path loss and slow fading, also known as shadowing. The main focus for this work has been on path loss and shadowing. The signal propagation model that is employed is shown as followed.

$$P_r(p) = \left(\frac{p}{p_0}\right)^{-\eta} \frac{P_t}{Pl(p_0)} \Phi, \tag{9}$$

where $P_r(p)$, P_t, p and η denote received signal strength (RRS), transmitted power, propagation distance and path-loss exponent respectively. The parameter p_0 denoted to the reference distance with a known path-loss, $Pl(p_0)$. The shadowing effect is modelled by the random variable, Φ, which follows a log-normal distribution such that $10log_{10}\Phi$ follows a zero mean Gaussian distribution with a standard deviation σ in dB.

3.2.2 Cell Edge Reliability

In cellular networks, a minimum signal strength γ is usually required to maintain the desired QoS. The cell edge reliability is defined as the probability that the received power strength measured on a circular contour at the desired cell edge will exceed or meet a desired quality

threshold. In addition, the reliability metric can also be defined for any point within the cell coverage, i.e. $\mathbb{P}\boldsymbol{r}[\boldsymbol{P_r}(\boldsymbol{p}) \geq \boldsymbol{\gamma}],\ \forall\ \boldsymbol{0} \leq \boldsymbol{p} \leq \boldsymbol{R}$, where $\boldsymbol{R}$ is the radius of the cell.

3.2.3 Cell Coverage Probability

The cell coverage probability, $\mathcal{C}$, is defined as the fraction of the cell area where the received power is above the minimum required signal strength γ. The cell coverage probability is obtained by integrating the contour probability over the entire coverage area of the cell, i.e. across all contours of the cell including the cell edge and dividing it by the cell area. Hence, the cell coverage probability is expressed as

$$\mathcal{C} = \frac{1}{\mathcal{A}} \int_{\mathcal{A}} p.P[P_r(p,\phi) \geq \gamma] dp\ d\phi\ , \tag{10}$$

where $\mathcal{A}$ denotes to the cell area illustrated in Figure 3.1. Single cell deployment has been considered for this work.

3.2.4 GPS Error Modelling

We consider that a central controller utilises GPS to estimate the position of each UE. The GPS system has an uncertainty region of radius ***r*** (as discussed in chapter 3.1), which implies that given the UE reported coordinates are ***(c, d)***, the actual UE position is a point with coordinates ***(x, y)*** that satisfies

$$(x-c)^2 + (y-d)^2 \leq r^2 \tag{11}$$

Considering a HetNet where the macro cells provide ubiquitous coverage while the small cells are for high data rate transmissions. Furthermore, the macro cells are aware of the exact position of the small cells and they allocate UEs to each small cell based on the GPS report of the UEs position.

As a result of the uncertainty in GPS estimations, some of the UEs might not be in the coverage of their allocated small cells.

3.3 Coverage Probability Estimation

In this section, the modified expression of the cell edge reliability and the cell coverage probability that take into consideration the GPS estimation error are derived. Firstly, for the simplified case without shadowing, and then we extend it for the shadowing case.

3.3.1 Case without Shadowing

When the GPS uncertainty and shadowing are neglected, the cell edge reliability and cell coverage probability and equivalent and can be expressed as in (12).

$$\mathbb{P}r[P_r(p) \geq \gamma] \equiv \mathcal{C} = \begin{cases} 1, & p \leq p_0 \left(\dfrac{\gamma\, Pl(p_0)}{P_t}\right)^{\eta} \\ 0, & p > p_0 \left(\dfrac{\gamma\, Pl(p_0)}{P_t}\right)^{\eta} \end{cases} \tag{12}$$

When the GPS uncertainty is considered, in order to estimate the cell edge reliability, we need to estimate the area of all possible UE positions. Given the cell centre coordinates, ***(a, b)***, cell coverage radius, $\boldsymbol{R = p_0(\gamma Pl(p_0)/P_t)^{\eta}}$, and the reported UE coordinates, ***(c, d)***; we are interested in finding the area of the dotted circle that lies within the cell coverage as illustrated

in FIGURE 3.1. By using laws of trigonometry and equations derived in section 3.1, the area is obtained as shown in (13).

$$\bar{A} = \begin{cases} \pi r^2, & 0 < p \leq R - r \\ \pi r^2 - \left[\dfrac{(\beta - \sin\beta)r^2}{2} - \dfrac{(\theta - \sin\theta)R^2}{2}\right], & R - r < p \leq \sqrt{R^2 - r^2} \\ \left[\dfrac{(\beta - \sin\beta)r^2}{2}\right] + \left[\dfrac{(\theta - \sin\theta)R^2}{2}\right], & \sqrt{R^2 - r^2} < p < R \end{cases} \tag{13}$$

The parameter ***p*** is the distance between the reported UE position and the cell centre (1). Consequently, the reliability of the received signal at any point in the interval $\boldsymbol{0 \leq p \leq R}$ can be expressed as

$$\begin{aligned} \mathbb{P}r[P_r(p) \geq \gamma] &= \frac{\bar{A}}{\pi r^2} \\ &\equiv \begin{cases} 1, & 0 < p \leq R - r \\ 1 - \left[\dfrac{(\beta - \sin\beta)}{2\pi} - \dfrac{(\theta - \sin\theta)}{2\pi}\left(\dfrac{R}{r}\right)^2\right], & R - r < p \leq \sqrt{R^2 - r^2} \\ \dfrac{(\beta - \sin\beta)}{2\pi} + \dfrac{(\theta - \sin\theta)}{2\pi}\left(\dfrac{R}{r}\right)^2, & \sqrt{R^2 - r^2} < p < R \end{cases}, \end{aligned} \tag{14}$$

for the case without shadowing.

This clearly shows that 100% reliability is only obtained when the reported UE position is at a distance such that $\boldsymbol{0 \leq p \leq R\text{-}r}$. Therefore, the cell area coverage probability according to (2) as,

$$\begin{aligned} \mathcal{C}_{ns} = {} & \frac{R^2 - (R - r)^2}{R^2} \\ & + \frac{1}{\pi R^2}\left(\int_{R-r}^{\sqrt{R^2-r^2}} p(1 - \bar{A}_1)dp + \int_{\sqrt{R^2-r^2}}^{R} p(\bar{A}_1 + 2\bar{A}_2)dp\right) \end{aligned} \tag{15}$$

for the case without shadowing, where $\bar{A}_1$ and $\bar{A}_2$ are defined as followed in (16) and (17) respectively.

$$\bar{A}_1 = \frac{(\beta - \sin\beta)}{2\pi} - \frac{(\theta - \sin\theta)}{2\pi}\left(\frac{R}{r}\right)^2 \tag{16}$$

and,

$$\bar{A}_2 = \frac{\theta - \sin\theta}{2\pi}\left(\frac{R}{r}\right)^2 \tag{17}$$

with θ and β defined in (2) and (3) respectively.

Note that the modified reliability and coverage probability expressions in (14) and (15) respectively, reverts to the expression in (12) when the GPS error radius r is zero, $\boldsymbol{r} = \boldsymbol{o}$.

3.3.2 Case with Shadowing

Here we consider the scenario where both shadowing and path-loss are the dominant factors in the channel propagation model. The probability that the reported received signal strength (RSS) (in dB) at a distance $\boldsymbol{p}$ from the base station will exceed the threshold γ, i.e., $\mathbb{P}\boldsymbol{r}[\boldsymbol{P_r}(\boldsymbol{p}) \geq \boldsymbol{\gamma}]$ can be obtained from [81] and [82] as in (18).

$$\mathbb{P}r[P_r(p) \geq \gamma] = \frac{1}{2} - \frac{1}{2}\, erf\left(a + b\ln\frac{p}{R}\right) \tag{18}$$

In the same way, the cell coverage probability without the error in location information can be expressed as in (19).

$$\mathcal{C} = \frac{1}{2} - \frac{1}{R^2}\int_0^R p.erf\left(a + b\ln\frac{p}{R}\right)dp \tag{19}$$

where a and b are defined in (20) and (21) as shown below.

$$a = \frac{\left(\gamma(dBm) - P_t(dBm) + Pl(p_o)(dB) + 10\eta\log_{10}\frac{R}{p_o}\right)}{\sigma\sqrt{2}} \tag{20}$$

and,

$$b = 10\eta\log_{10} e/\sigma\sqrt{2} \tag{21}$$

when there is no error in UE location information.

Given the reliability expression in (18), now we consider the case with error in the geographical location information reported by the UE to their serving BS. As stated earlier, the actual location of a UE lies within a circular disc centred at the reported location. Consequently, its actual location with reference to its reported location can modelled as

$$\bar{p}(\kappa, \phi) = \sqrt{p^2 + \kappa^2 - 2p\kappa\cos\phi} \tag{22}$$

such that $\boldsymbol{0 \leq \kappa \leq r}$ and $\boldsymbol{0 \leq \phi \leq 2\pi}$ defines every possible point due to GPS error. The PDF of the distance and the direction of UE's actual location with respect to its reported position are $\frac{1}{r}$ and $\frac{1}{2\pi}$, respectively. Therefore, the modified $\mathbb{P}\boldsymbol{r}[\boldsymbol{P_r(p)} \geq \boldsymbol{\gamma}]$ as a result of the inaccuracies in the UE's location information can be obtained as in (23).

$$\begin{aligned}\overline{\mathbb{P}r_s[P_r(p) \geq \gamma]} &= \mathbb{E}_{\kappa,\phi}\{\mathbb{P}\mathrm{r}[\mathrm{P_r}(\bar{\mathrm{p}}(\kappa, \phi)) \geq \gamma]\} \\ &= \frac{1}{2\pi r}\int_0^r \int_0^{2\pi} \mathbb{P}\mathrm{r}[\mathrm{P_r}(\bar{\mathrm{p}}(\kappa, \phi)) \geq \gamma]\, d\phi d\kappa\end{aligned} \tag{23}$$

where $\mathbb{E}$ is the expectation. This further simplifies as

$$\overline{\mathbb{P}r_s[P_r(p) \geq \gamma]} = \frac{1}{2\pi r}\int_0^r \int_0^{2\pi} \left[\frac{1}{2} - \frac{1}{2}\, erf\left(a + \frac{b}{2}\ln\frac{(\bar{p}(\kappa,\phi))^2}{R^2}\right)\right] d\phi d\kappa \tag{24}$$

by substituting (18) into (23). consequently, the actual percentage of the area $\mathcal{A}$ in coverage when the shadowing is considered, can be expressed according to (10) as shown below in (25).

$$\begin{aligned}\mathcal{C}_s &= \frac{1}{\mathcal{A}}\int \overline{\mathbb{P}r_s[P_r(p) \geq \gamma]}\, d\mathcal{A} \\ &= \frac{1}{\pi r R^2}\int_0^R \int_0^r \int_0^{2\pi} p\left[\frac{1}{2}\right. \\ &\quad \left. - \frac{1}{2}\, erf\left(a + \frac{b}{2}\ln\frac{(\bar{p}(\kappa,\phi))^2}{R^2}\right)\right] d\phi d\kappa dp\end{aligned} \tag{25}$$

The modified reliability expression and coverage probability derived in (24) and (25) respectively for the case where the GPS error and shadowing were considered, revert back to the expression (18) and (19), when the GPS error radius is zero, r = 0, since κ and ϕ will also be zero.

3.4 Numerical Results and Discussions

In this section, we verify the accuracy of our modified reliability and the cell coverage probability expressions that were derived for both shadowing and non-shadowing cases numerically.

For the purpose of this work, we consider the scenario with a single base station transmitting at a fixed power, $\boldsymbol{P_t = 46\ dBm}$. Also, we assume that the minimum received signal that the UE can effectively decode is $\boldsymbol{P_{min} = -84.5\ dBm}$. Hence, we obtain the cell coverage radius, $\boldsymbol{R}$, from (9) with $\Phi = 1$ and by using the parameters in **Table I** [83].

Table I - List of Parameters

Parameters	Symbol	Value (unit)
Standard Deviation	σ	7
Path-loss Exponent	η	3.5
Reference Distance	P_0	1m
Path-loss at p_0	$Pl(p_0)$	34.5dB
Power Transmitted	P_t	46dBm
Threshold	γ	-84.5dBm

For MATLAB simulation, 100,000 UEs are randomly positioned within the coverage of the cell, to represent the reported positions. We incorporate the GPS error to the reported position of each UE by adding a random displacement, $\boldsymbol{(\acute{r}_i, \delta)}$, for each UE, such that $\boldsymbol{0 \leq \acute{r}_i \leq r}$, and $\boldsymbol{0 \leq \delta \leq 2\pi}$ to obtain the exact UE position.

For the case without shadowing, in order to verify the coverage probability $\boldsymbol{\mathcal{C}_{ns}}$ in (15), we simply evaluate the signal strength at exact UE position, i.e. $\boldsymbol{P_r}$, using (9) with $\boldsymbol{\Phi} = 1$. Therefore, we obtain the percentage of UE with $\boldsymbol{P_r \geq \gamma}$, which refers to as the simulation approach coverage probability.

In FIGURE 3.4, the exact coverage probability obtained from (15) and the coverage probability using the simulation approach for GPS approximation radius, ***r***, ranging from 5 to 100, when shadowing is not considered is compared. As it can be seen in the figure, the GPS error modified coverage probability expression tightly matches with the simulation approach.

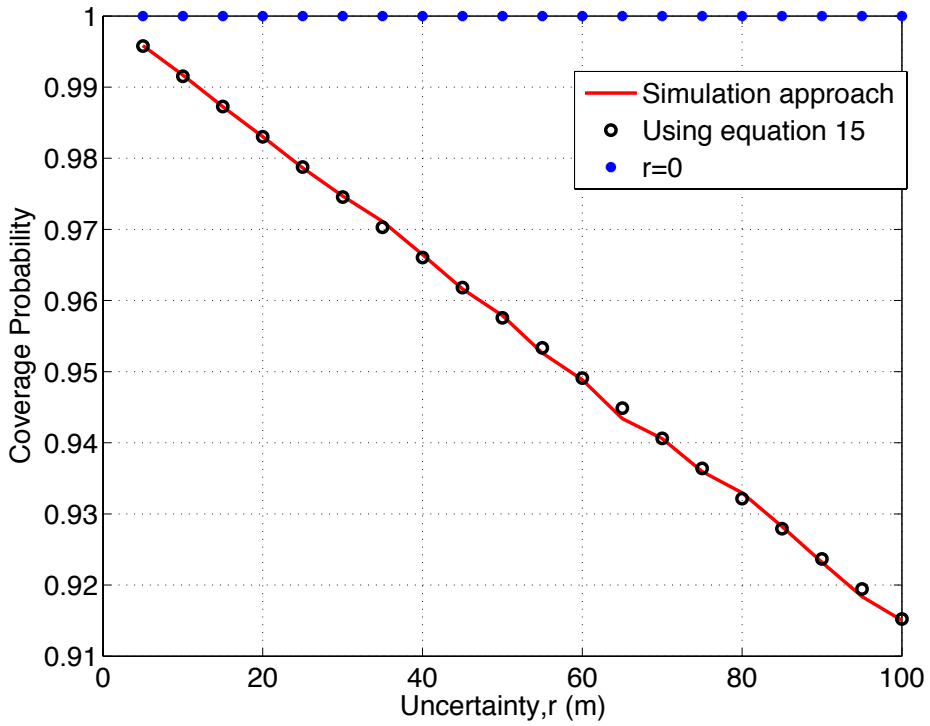

FIGURE 3.4: The coverage probability as a fraction of GPS error radius when shadowing is not considered.

Furthermore, it can be seen that the coverage probability reduces linearly with the GPS error radius. At r = 20m, approximately ***2%*** of the UE will be out of coverage, which is further degraded to about ***6%*** at $r = 70m$. Hence, the GPS error results into coverage gaps in the network. It can also be observed that as GPS radius $r \rightarrow 0$, the coverage probability $\mathcal{C}_{ns} \rightarrow 1$, which is as expected.

For the case with GPS error and shadowing, in order to get more accurate results, 10,000,000 UEs are randomly positioned within the coverage of the cell, to represent the reported position. Similar to the previous (non-shadowing) case, the simulation approach coverage probability is

obtained by finding the percentage of UEs with $P_r \geq \gamma$, where P_r calculated from (9) and $10log_{10}\Phi$ follows a zero mean Gaussian distribution with standard deviation σ. The results (FIGURE 3.5) shows that, while shadowing in considered, the GPS error modified coverage probability in (25) matches tightly with the simulation approach.

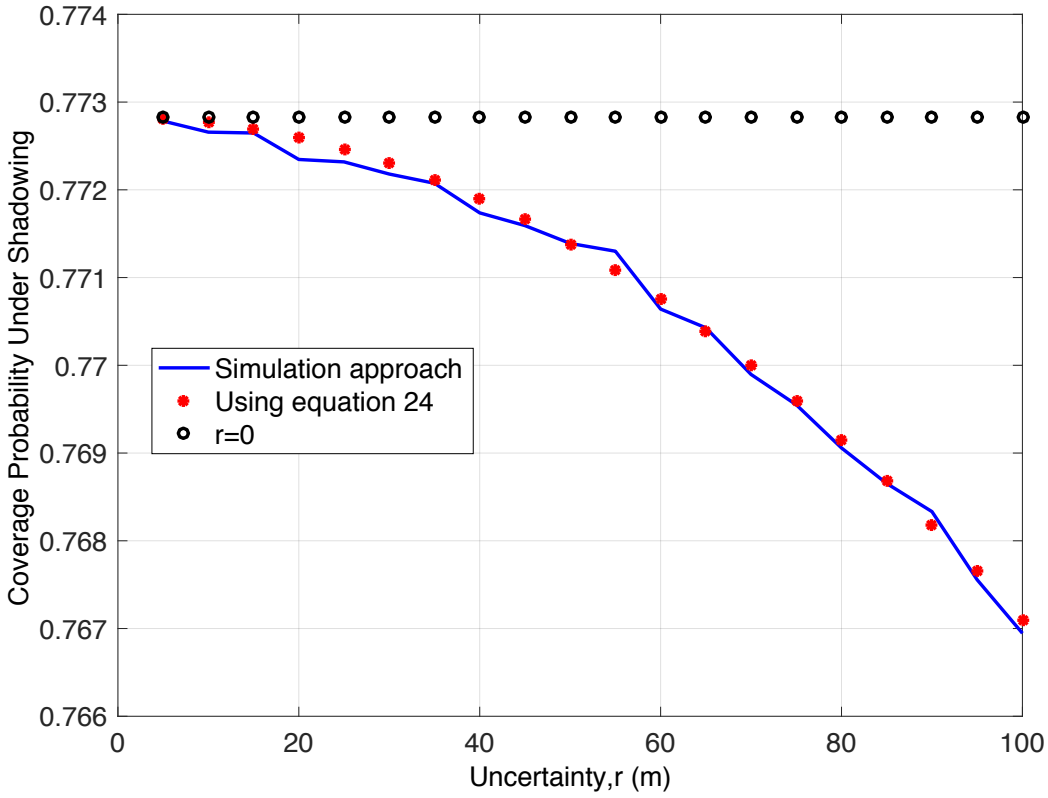

FIGURE 3.5: The coverage probability of the user under shadowing for different uncertainties (r).

Similar to the non-shadowing case, the coverage probability reduces with the GPS error radius. Also, the GPS error results into coverage gaps in the network, since the coverage probability with GPS error, i.e. $r > 0$, is lower than that without GPS error, i.e. $r = 0$. It can also be seen that as the GPS error radius $r \rightarrow 0$, the coverage probability $C_s \rightarrow C$ in (19), which is as expected.

Figure 3.6 shows the plot of the performance degradation (PD), as a result of GPS error, for shadowing standard deviations $\sigma = 7,9$ and $12dB$. The performance degradation is defined as $PD = (\mathcal{C}_s - \mathcal{C})/\mathcal{C}$, where $\mathcal{C}$ defined in (19) is the cell coverage probability for the shadowing case without GPS error.

It can be seen in FIGURE 3.6 that the performance becomes more degraded as the shadowing standard deviation σ reduces. This implies that the GPS approximation error is less severe on the coverage as σ increases. This is due to the fact that by increasing σ, more randomness is introduced to the received signal; hence, uncertainty/randomness created by the GPS error would have more impact on a lower σ.

FIGURE 3.7 shows the plot of the reliability of the RF signal received by the UE positioned at a distance p from the centre of the cell, i.e. $\mathbb{P}r[P_r(p) \geq \gamma]$ such that $0 \leq p \leq R$, $\gamma = -84.5dBm$, $\sigma = 7dB$ and $r = 50$, for both the shadowing and non-shadowing cases.

For the non-shadowing case with GPS error, it can be seen that the reliability, $\mathbb{P}r_{ns}[P_r(p) \geq \gamma] = 1$ when $p \leq R-r$, and depreciates from this value when $p > R-r$. Whereas, $\mathbb{P}r[P_r(p) \geq \gamma] = 1, \forall\, 0 \leq p \leq R$, when there is no GPS error and shadowing.

For the case with shadowing, as it's shown in FIGURE 3.7, the reliability $\mathbb{P}r_s[P_r(p)]$ obtained when there is GPS error is always less than the reliability without GPS error.

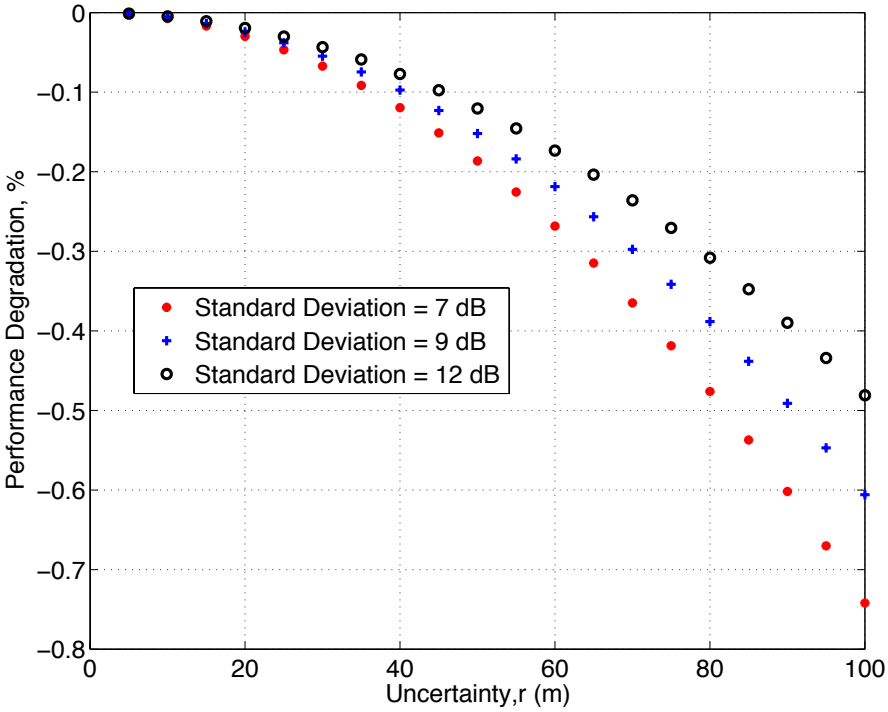

FIGURE 3.6: Coverage degradation as a result of GPS error.

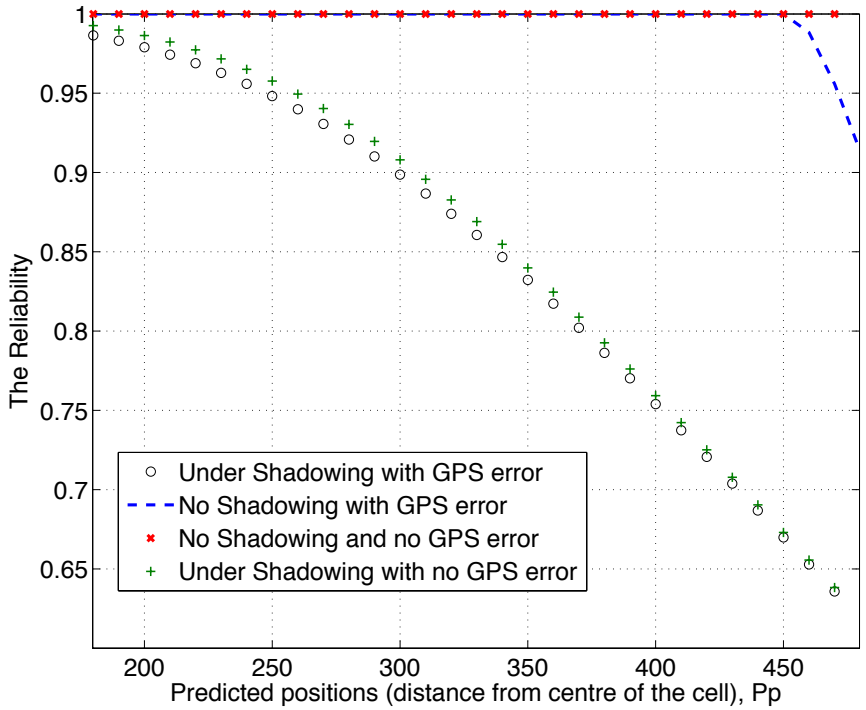

FIGURE 3.7: Reliability of UE at a distance p from the cell centre, for the shadowing and non-shadowing cases.

Summary

In this chapter, the preliminary investigations on enabling SON is provided. The impact of user geographical positioning error (GPS error) on the cell coverage is investigated. A single cell scenario is considered in which the cell coverage probability estimation for both the path-loss only channel model and when shadowing is added is derived. Some of the results in this chapter were published in [19].

CHAPTER 4

4 Coverage Estimation Considering User and Access Point Position Uncertainty

In this chapter, the effect of inaccurate user and base station position estimation (GPS error) on the cell coverage is investigated. A single cell scenario is considered in which the cell edge and coverage probabilities for both shadowing and non-shadowing cases are derived.

4.1 Autonomous Coverage Estimation Framework

We consider an autonomous coverage estimation (ACE) scheme which exploits the measurement reports gathered by the UEs. In such a system, UEs measurement reports are tagged with their geographical location information and sent to their serving base station. The serving base station after retrieving the measurements, further appends its geographical location information and forwards them to a trace collection entity (TCE), which can then generate the coverage map.

The reported geographical coordinates of the UEs and base stations are obtained from positioning techniques, such as observed time difference of arrival (OTDOA) or assisted global positioning system (A-GPS) [15], [16]. However, these techniques are prone to errors, and, hence the reports may be tagged to a wrong location. In this chapter, given a reported UE

position, ***o***, with coordinates ***(c, d)***, we assume that its actual location is within a circular disc with radius ***r*** which is cantered at ***o***, as illustrated in FIGURE 3.1(a). Furthermore, we assume that errors in base station positioning can be resolved such that its displacement from its reported position, ***e***, is known.

For analytical tractability, we consider a single cell deployment scenario where RSS measurement reports are gathered by the UE. The signal propagation model we employ for obtaining the RSS is as shown in (9).

The error in coverage estimation due to such autonomous scheme is evaluated by assessing the reliability of radio frequency (RF) coverage on the measurement based on the fundamental metric of cell coverage probability.

4.1.1 Cell Coverage Probability

In general, the cell coverage probability can be defined as,

$$\mathcal{C} = \frac{1}{\mathcal{A}} \int \mathbb{P}r[P_r(p) \geq \gamma] \, d\mathcal{A} \tag{26}$$

and can be thought of equivalently as the average fraction of the UE who at any time achieves a target reference signal received power (RSRP), γ, i.e. the average fraction of network area that is in coverage at any time. Hence, given a circular radial distance ***R*** from the base station, we are interested in computing the percentage of area with RSRP greater than or equal to γ.

4.1.2 Error in Coverage Estimation via ACE

The cell coverage probability obtained from (26) will be the same as the ACE scheme when the tagged geographical location information's are accurate. However, the ACE scheme becomes sub-optimal when the reported UE and base station positions deviate from the actual, thus leading to a much lower cell coverage probability. Hence, we define the error in coverage estimation via ACE, which quantifies how its estimated coverage probability deviates from the actual cell coverage probability over a fixed area, as followed in (27).

$$\mathcal{D}_A = \left| \frac{\mathcal{C} - \mathcal{C}_{ACE}}{\mathcal{C}} \right| * 100\% \tag{27}$$

where $\mathcal{C}$ and $\mathcal{C}_{\text{ACE}}$ are the actual cell coverage probability given in (26) and the coverage probability estimated from the ACE scheme, respectively, over a fixed area, $\mathcal{A}$. In the following section, we derive the coverage probability of the ACE scheme.

4.2 Cell Coverage Probability with ACE

In this section, the modified expression for the actual coverage probability from the ACE scheme is derived when there are errors in UE and base station geographical location information. Firstly for the case with shadowing in addition to path-loss, and then for the path-loss only channel model.

4.2.1 ACE Coverage Probability: Path-Loss and Shadowing Channel Model

Here we consider the scenario where both shadowing and path-loss are the dominant factors in the channel propagation model. The probability that the reported RSRP (in dB) at a distance $\boldsymbol{p}$ from the base station will exceed the threshold γ, i.e., $\mathbb{P}\boldsymbol{r}[\boldsymbol{P_r}(\boldsymbol{p}) \geq \boldsymbol{\gamma}]$ as shown in (18), when there are no error in UE and base station location information. In the same way, the cell coverage probability of the ACE scheme without error in location information is shown in (19).

In addition to the UE's position error (considered in chapter 3), we consider here the scenario where the geographical location information reported by the serving base station to the TCE is displaced at a distance $\boldsymbol{e}$ from its actual location, as depicted in FIGURE 4.1. Hence, the measurement reports stored in the TCE are also tagged with a wrong base station position, thus resulting in the generation of a wrong coverage map. In order to estimate the actual coverage probability of the ACE scheme over the area $\mathcal{A}$ (circular area) centred at the reported base station position X, we estimate the fraction of the measurement reports that will still be in coverage based on the actual base station position $\bar{X}$.

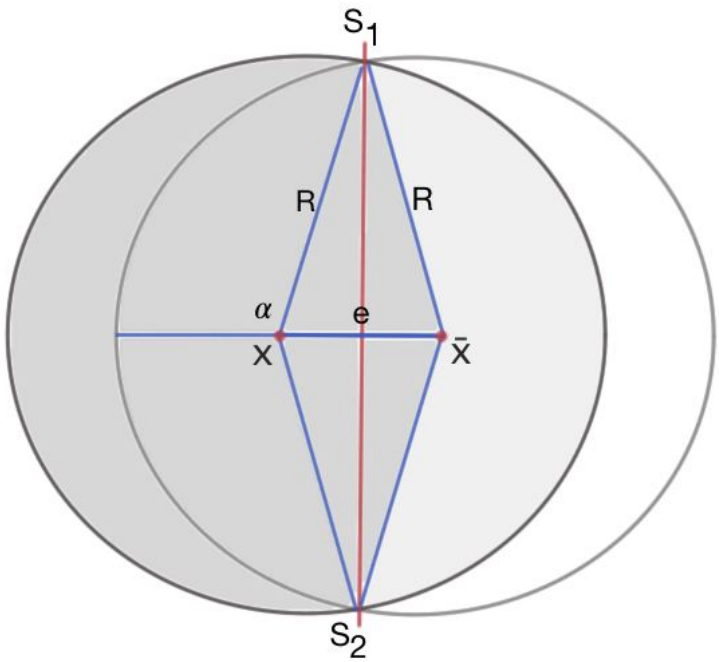

FIGURE 4.1: Base station with reported position at *X* has an actual location $\bar{X}$, which is displaced from *X* by e.

Consider R as the radius of the area of interest $\mathcal{A}$ centred at X, we can create a virtual representation of $\mathcal{A}$ centred at $\bar{X}$ such that both intersects at S_1 and S_2, as shown in FIGURE 4.1. The intersecting points are characterised by the angle α, $\alpha = \pi - \cos^{-1}\left(\frac{e}{2R}\right)$. Hence, using this property, we define two regions, $\mathcal{A}_1$ and $\mathcal{A}_2$, which are the shaded and unshaded areas in the area of interest, respectively, and from that we estimate the actual fraction of UE in coverage based on the actual base station position $\bar{X}$.

It can be noted that, the sum of the areas of the two regions $\mathcal{A}_1$ and $\mathcal{A}_2$ is equal to $\mathcal{A}$, $\mathcal{A}_1 + \mathcal{A}_2 = \mathcal{A}$.

The distance between the reported UE position in region $\mathcal{A}_1$ and $\mathcal{A}_2$ with respect to the actual base station positions can be expressed as followed in (28) and (29) respectively.

$$\tilde{p}_{\mathcal{A}_1}(\theta) = \sqrt{R^2 + e^2 - 2Re\cos\left[\pi - \theta - \sin^{-1}\left(\frac{e\sin\theta}{R}\right)\right]} \tag{28}$$

$$\tilde{p}_{\mathcal{A}_2}(\theta) = \sin\left[\theta - \sin^{-1}\left(\frac{e\sin(\pi-\theta)}{R}\right)\right]\left[\frac{\sin(\pi-\theta)}{R}\right]^{-1} \tag{29}$$

where $\boldsymbol{\pi - \alpha \leq \theta \leq 2\pi - \alpha}$ and $\boldsymbol{2\pi - \alpha \leq \theta \leq 3\pi - \alpha}$ for $\boldsymbol{\tilde{p}_{\mathcal{A}_1}(\theta)}$ and $\boldsymbol{\tilde{p}_{\mathcal{A}_2}(\theta)}$ respectively.

Consequently, the actual coverage probability of the ACE scheme over the area $\mathcal{A}$ can be expressed as in (30)

$$\begin{aligned} C_{ACE} = \frac{2}{\pi R^2}\Bigg(&\int_0^{\pi-\alpha}\int_0^{\tilde{p}_{\mathcal{A}_1}(\theta)} p\overline{\mathbb{P}r[P_r(p) \geq \gamma]}\, dp d\theta \\ &+ \int_0^{\alpha}\int_0^{\tilde{p}_{\mathcal{A}_2}(\theta)} p\overline{\mathbb{P}r[P_r(p) \geq \gamma]}\, dp d\theta\Bigg) \end{aligned} \tag{30}$$

when there are errors in both UE and base station geographical location information.

By substituting the expression of $\overline{\mathbb{P}r[P_r(p) \geq \gamma]}$ in (24) into (30), the actual coverage probability of the ACE scheme can be further expressed as (31).

$$\begin{aligned} \mathcal{C}_{ACE} = \frac{2}{\pi R^2}\Bigg(&\int_0^{\pi-\alpha}\int_0^{\tilde{p}\mathcal{A}_1(\theta)}\int_0^{r}\int_0^{2\pi} p\left[\frac{1}{2}\right. \\ &\left. -\frac{1}{2}\, erf\left(a+\frac{b}{2}\ln\frac{(\bar{p}(\kappa,\phi))^2}{R^2}\right)\right] d\phi d\kappa\, dp d\theta \\ &+\int_0^{\alpha}\int_0^{\tilde{p}\mathcal{A}_2(\theta)}\int_0^{r}\int_0^{2\pi} p\left[\frac{1}{2}\right. \\ &\left. -\frac{1}{2}\, erf\left(a+\frac{b}{2}\ln\frac{(\bar{p}(\kappa,\phi))^2}{R^2}\right)\right] d\phi d\kappa\, dp d\theta\Bigg) \end{aligned} \tag{31}$$

4.2.2 ACE Coverage Probability: Path-Loss Only Channel Model

Here we consider the scenario where the path-loss is the prominent factor in channel propagation model. We further assume that the cell coverage radius $\boldsymbol{R}$ is such that $\boldsymbol{R} = \boldsymbol{p_0}\left(\frac{\boldsymbol{\gamma P l(p_0)}}{\boldsymbol{P_t}}\right)^{\boldsymbol{\eta}}$. Hence, for the case with no error in geographical location information and no shadowing, $\mathbb{P}r[P_r(p) \geq \gamma] = 1$, while $\boldsymbol{0} \leq \boldsymbol{p} \leq \boldsymbol{R}$. Consequently from (26), in this case, the cell coverage probability over the circular radial distance, $\boldsymbol{R}$, is 1, $\mathcal{C} = 1$.

It can be seen that when we consider the path-loss only channel model and the base station error is neglected, $\overline{\mathbb{P}r[P_r(p) \geq \gamma]}$ in (23) is equivalent to the fraction of the circular disk that lies within the cell radius R (Figure 3.1). Hence, using some trigonometry, it can be obtained as (32), when $0 \leq p \leq R$. From (32), the coverage probability of it over the area $\mathcal{A}$ can be defined as (33) for when there's not shadowing and only the UE positioning error is considered.

$$\overline{\mathbb{P}r[P_r(p) \geq \gamma]} = \frac{\beta - \sin\beta}{2\pi} + \frac{\theta - \sin\theta}{2\pi}\left(\frac{R}{r}\right)^2 \tag{32}$$

$$\begin{aligned} \mathcal{C}_{ACE} &= \frac{1}{\mathcal{A}} \int \overline{\mathbb{P}r[P_r(p) \geq \gamma]}\, d\mathcal{A} \\ &= \frac{1}{\pi R^2} \int_0^{2\pi} \int_0^R p \left(\frac{\beta - \sin\beta}{2\pi} + \frac{\theta - \sin\theta}{2\pi}\left(\frac{R}{r}\right)^2 \right) dp \end{aligned} \tag{33}$$

Following a similar approach with the shadowing case, we derive the cell coverage probability for the case with errors in both the UE and base station geographical location information. The cell coverage probability of the ACE for the case with path-loss as the dominant factor in the channel propagation model can also be expressed as in (30), but with $\overline{\mathbb{P}r[P_r(p) \geq \gamma]}$ defined for the non-shadowing case as $\overline{\mathbb{P}r[P_r(p) \geq \gamma]} = \frac{\beta - \sin\beta}{2\pi} + \frac{\theta - \sin\theta}{2\pi}\left(\frac{R}{r}\right)^2$. We thus arrive at (34).

$$\begin{aligned} \mathcal{C}_{ACE} = \frac{2}{\pi R^2} \Bigg(& \int_0^{\pi-\alpha} \int_0^{\tilde{p}\mathcal{A}_1(\theta)} p \left(\frac{\beta - \sin\beta}{2\pi} + \frac{\theta - \sin\theta}{2\pi}\left(\frac{R}{r}\right)^2 \right) dp d\theta \\ & + \int_0^{\alpha} \int_0^{\tilde{p}\mathcal{A}_2(\theta)} p \left(\frac{\beta - \sin\beta}{2\pi} + \frac{\theta - \sin\theta}{2\pi}\left(\frac{R}{r}\right)^2 \right) dp d\theta \Bigg) \end{aligned} \tag{34}$$

4.3 Numerical Results and Discussions

In this section, we present numerical results to verify the accuracy of the proposed analytical methodology against simulations, as well as to show the impact of errors in reported geographical location information on the actual coverage estimated by the ACE scheme. We consider measurement reports gathered for a single cell, with the parameters specified in **Table II** [83] and we estimate the cell coverage probability over a circular coverage region of area πR^2, where $R = p_0 \left(\frac{\gamma Pl(p_0)}{P_t}\right)^{\eta} \approx 553.1681$ m.

For the simulation part, 1,000,000 UEs are distributed following a uniform distribution over the circular cell region of radius R around the base station and their positions are taken as reported positions.

The actual position of the i^{th} UE with coordinated (c_i, d_i) is generated as $\left(c_i + r\sqrt{u_i}\cos(2\pi v_i), d_i + r\sqrt{u_i}\sin(2\pi v_i)\right)$. This is where u_i and v_i are pseudo random, pseudo independent numbers uniformly distributed in [0,1].

For the part with base station position error, the actual coordinates of the base station are obtained using the error e; such that if the reported coordinates were (x, y), the actual coordinates would be obtained as ($x+e$, y).

The RSRP at the actual generated UE position $P_r(\bar{p})$, is estimated according to (9) based on the distance between the actual base station and UE positions; where for the path-loss only channel model, Φ =1.

The cell coverage probability from the ACE scheme is then evaluated as the percentage of UE with $P_r(\bar{p}) \geq \gamma$.

Table II - List of Parameters

Parameters	Symbol	Value (unit)
Standard Deviation	σ	7,9,12 dB
Path-loss Exponent	η	3.5
Reference Distance	P_0	1m
Path-loss at p_0	$Pl(p_0)$	34.5dB
Power Transmitted	P_t	46dBm
Threshold	γ	-84.5dBm
UE Position Error	r	10-100m
Base Station Position Error	e	20m

In FIGURE 4.2 and FIGURE 4.3, we validate the derived cell coverage probability expressions of the ACE scheme for both cases of having only error in UE geographical location information, and when we have error in base station geographical location information in

addition to the error in UE geographical location information; and compare them. For both these figures, the base station (user deployed cell) position error has been fixed to 20. Since we have only considered one BS, the error is fixed with respect to all UEs (so no need for angle in BS error).

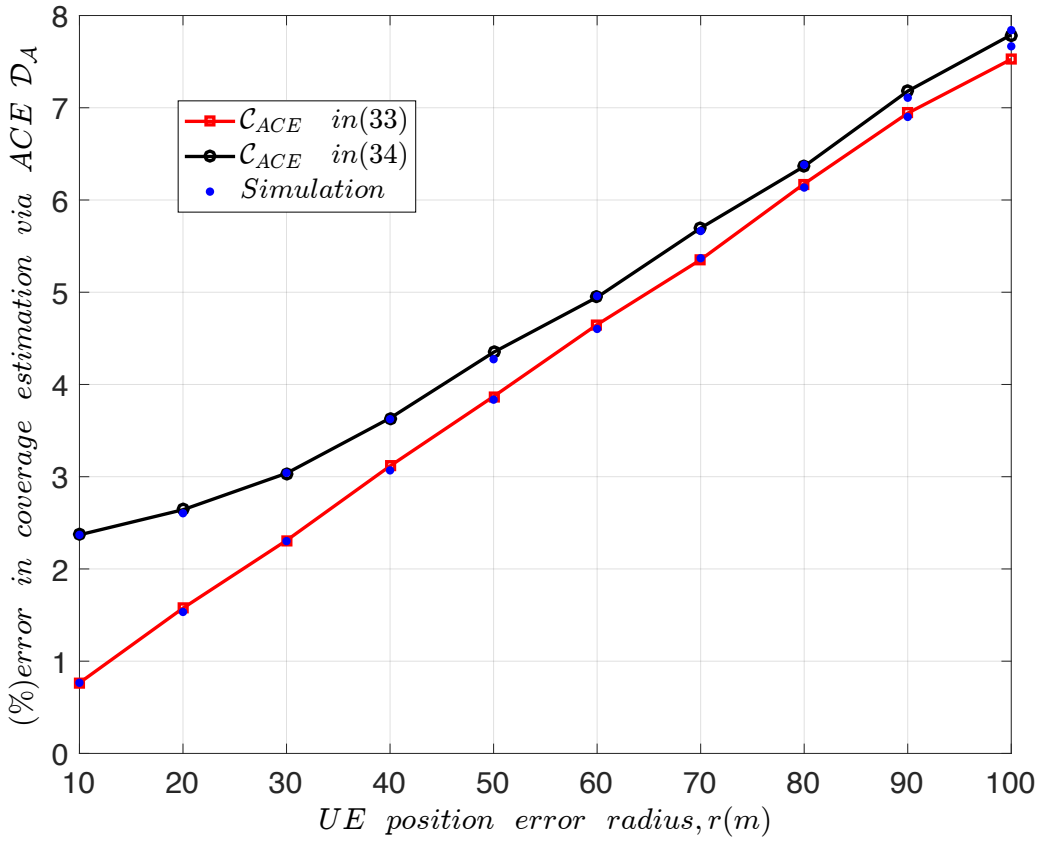

FIGURE 4.2: Error in coverage estimated via ACE for the path-loss only case, with e=20 in (34).

In FIGURE 4.3, we compare our analytical results on the error in coverage with ACE scheme over the area $\mathcal{A} = \pi R^2$, i.e., $\mathcal{D}_{\mathcal{A}}$, with the simulated results, for the case when path-loss and shadowing are the dominant factors in the signal propagation model. Whereas, a comparison for the case with path-loss as the dominant factor is presented in FIGURE 4.2. We note that in both figures, our analytical results tightly match with the simulation.

The results in FIGURE 4.2 and FIGURE 4.3 further show that the estimated error in the cell coverage probability as measured by the ACE scheme increases as the UE position error increases. Furthermore, having errors in base station location information further degrades the performance of the ACE scheme.

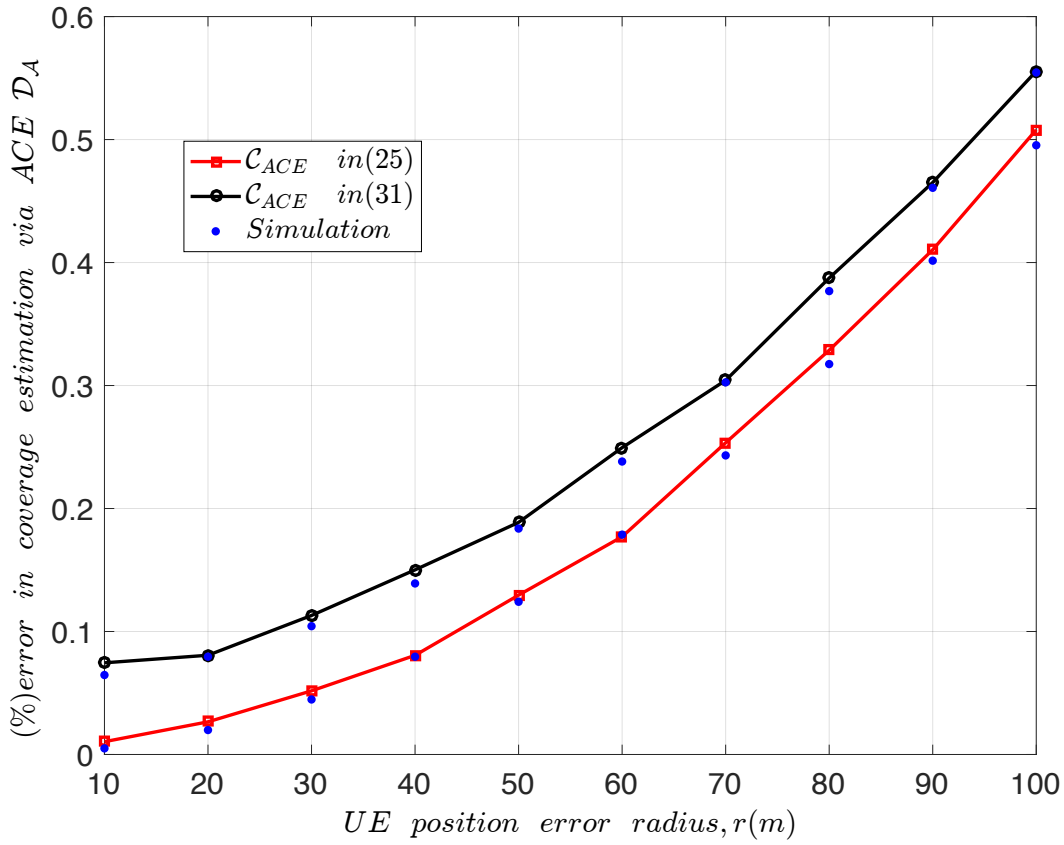

FIGURE 4.3: Error in coverage estimated via ACE when shadowing is considered in addition to the path-loss, with e=20 in (31).

FIGURE 4.4 shows the coverage probability at the reported UE position $\bar{p}$, which is at an angle θ to the reported base station position. For this case, the base station position error and the UE position error have been fixed on 100 m, i.e., e = 100 and r = 100.

It can be seen that the coverage probability obtained via the ACE scheme is much lower when there are errors in the base station and UE geographical location information, for the selected θ values.

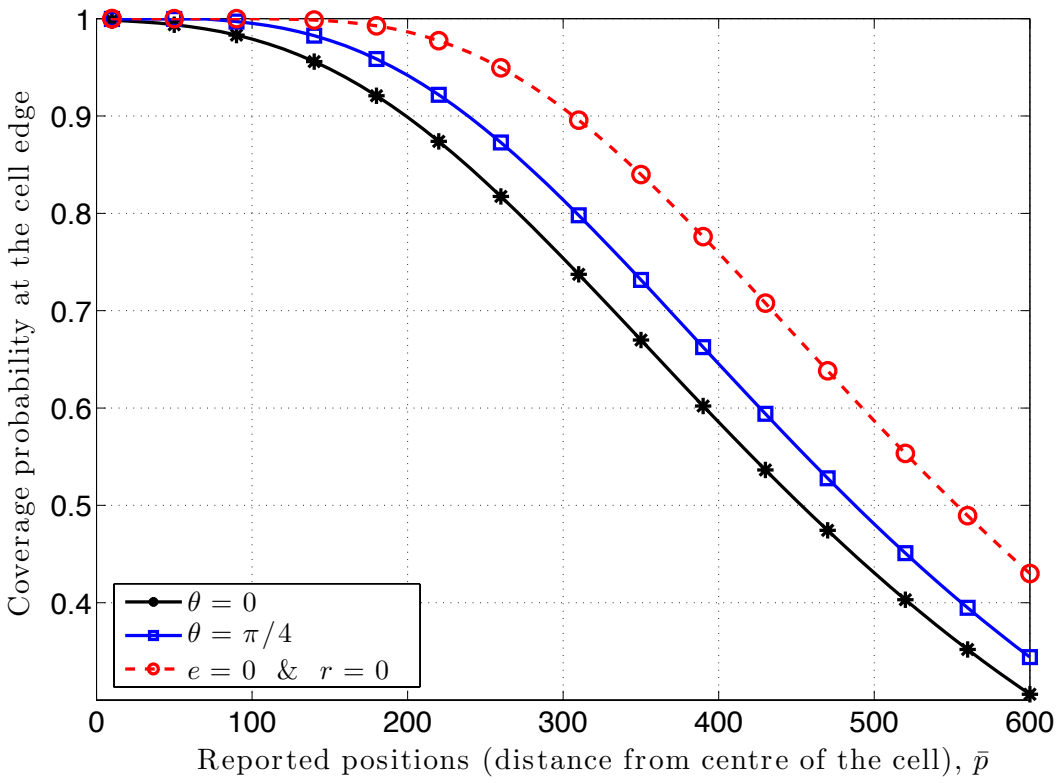

FIGURE 4.4: Coverage probability at the cell edge when e=100 and r=100.

In FIGURE 4.5, we plot the coverage estimation error as a result of using the ACE scheme, $\mathcal{D}_{\mathcal{A}}$, against the UE position error, for shadowing standard deviation σ = 7, 9, 12 dB and base station position error e = 0.20 m. We define the coverage estimation error, $\mathcal{D}_{\mathcal{A}}$, as in (27).

FIGURE 4.5 shows that the performance of the ACE scheme in estimating the actual coverage depreciates as the error in UE position increases. It can be seen that as the error in UE geographical location information increases, the percentage of error in coverage estimation via ACE increases. Furthermore, it can be observed that the performance of the ACE scheme becomes more degraded and the percentage error in the coverage estimation via ACE increases as the shadowing standard deviation σ reduces.

This implies that errors in UE and base station position estimations are less severe on the coverage as standard deviation σ increases. The reason for this is that increasing standard deviation σ introduces more randomness to the received signal; this results in the randomness created by the error in UE geographical location information to have more impact on a lower standard deviation σ.

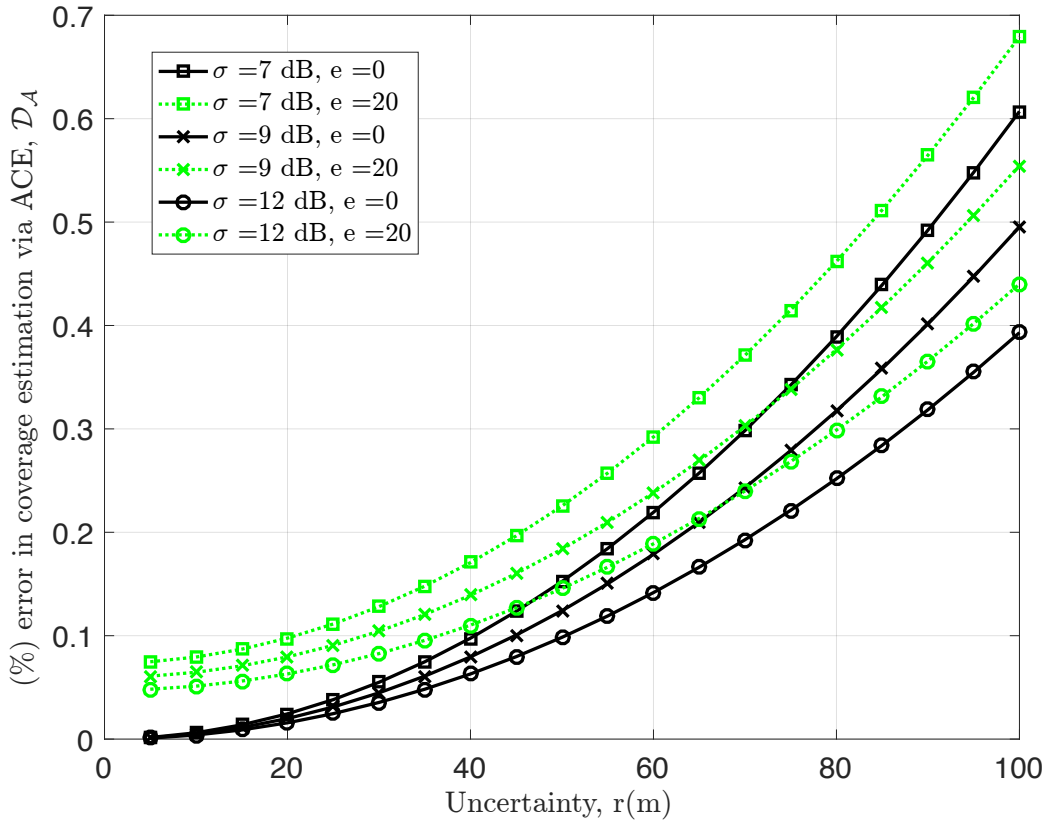

FIGURE 4.5: Cell Coverage Degradation with ACE.

In FIGURE 4.6 and FIGURE 4.7, we plot the 3D figure of the error in the coverage via ACE against UE position error radius, r, and base station position error, e. The results show that the performance of the ACE scheme depreciates as the error in the UE and base station geographical location information increases; this is the case for both the path-loss only channel model and when there's shadowing in addition to path-loss. It can be seen that as the error in

UE geographical location information increases, the percentage of error in coverage estimation via ACE increases.

In FIGURE 4.7, it can be further observed that the performance of the ACE scheme becomes more degraded as the shadowing standard deviation σ reduces.

This implies that the errors in UE and base station position estimations are less severe on the coverage as standard deviation σ increases. The reason for this is that increasing standard deviation σ introduces more randomness to the received signal; this results in the randomness created by the error in UE geographical location information to have more impact on a lower standard deviation σ.

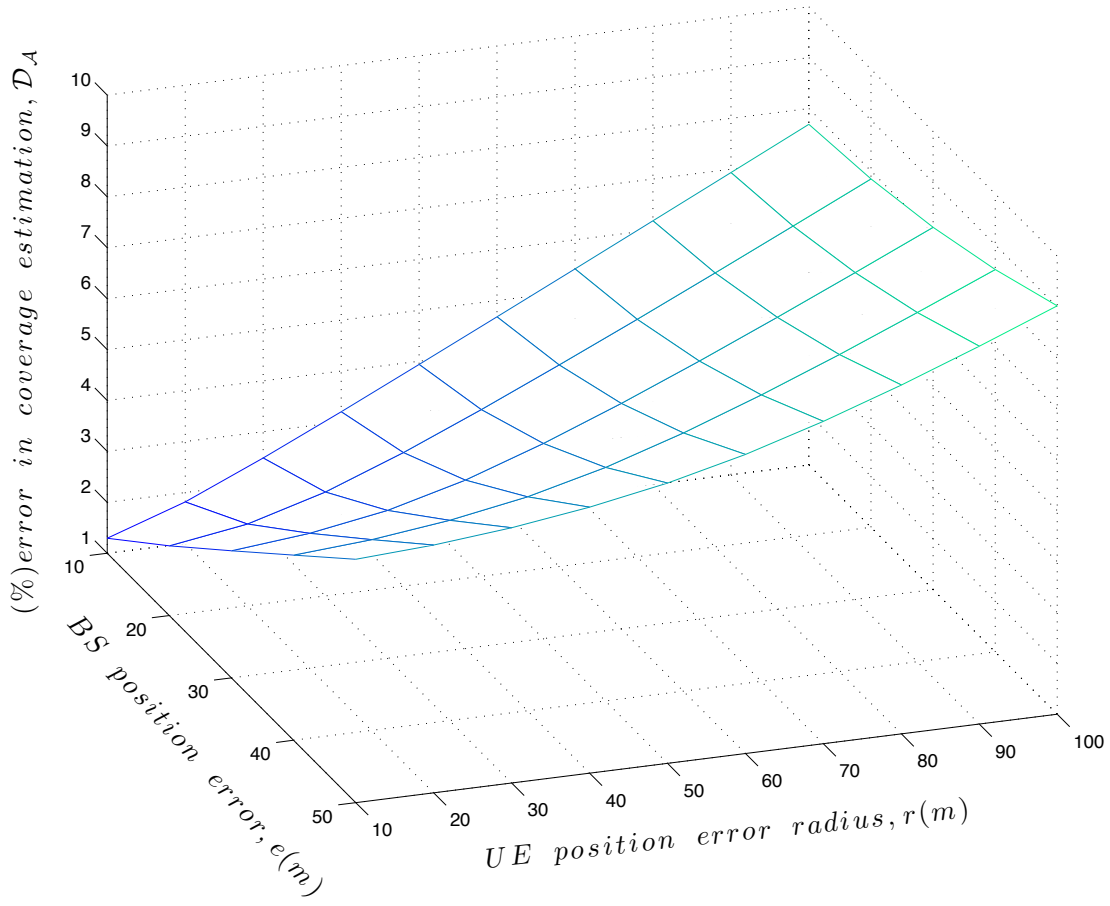

FIGURE 4.6: Error in Coverage Estimated via ACE: Path-loss only model.

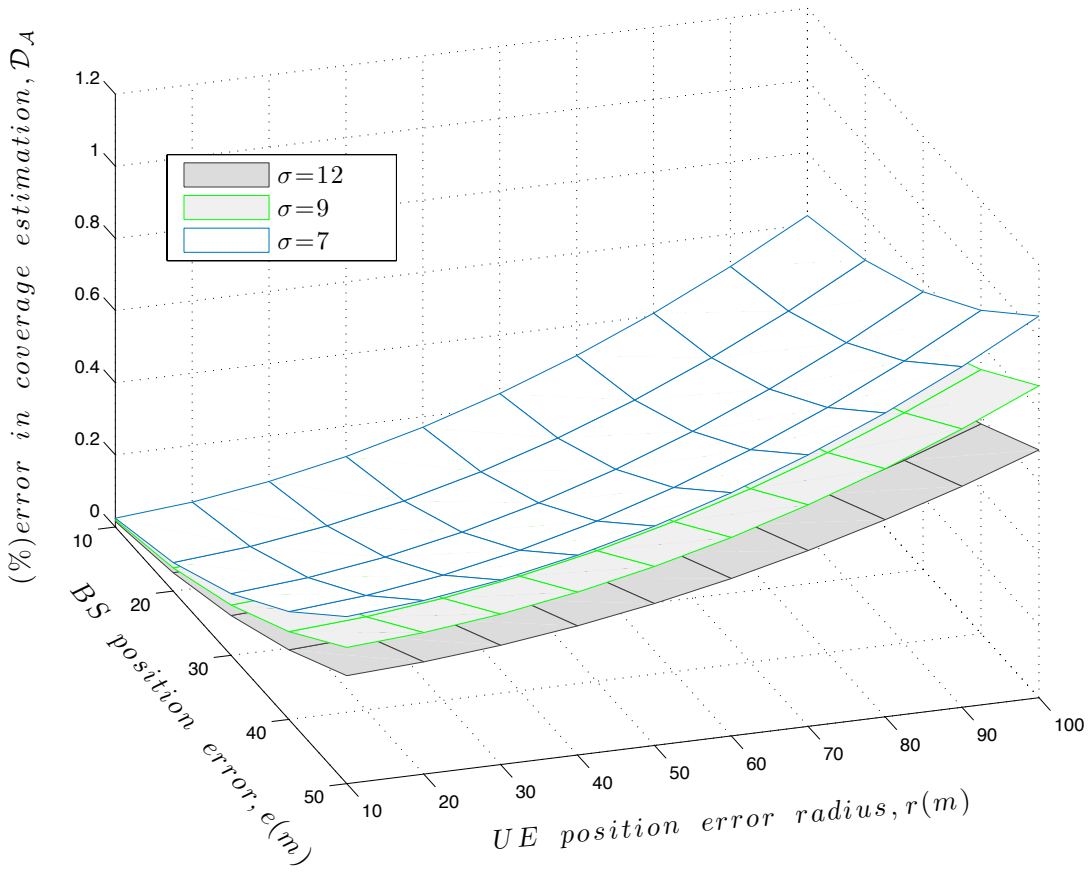

FIGURE 4.7: Error in Coverage Estimated via ACE: both Shadowing and Path-loss.

Summary

In this chapter, the effect of error in the user and base station geographical location information on the cell coverage estimation is investigated. An autonomous coverage estimation (ACE) schemes is introduced that exploits the measurement reports gathered by the UEs. The error in coverage estimation due to such autonomous scheme is evaluated by assessing the reliability of radio frequency (RF) coverage on the measurement based on the fundamental metric of cell coverage probability. This has been done for a single cell scenario and for both path-loss only channel model and the shadowing model. The results from this chapter have been published in [20] and [21].

CHAPTER 5

5 Sectored Cell ACE

In this chapter, the effect of inaccurate user and base station position estimation (GPS error) on the cell coverage is investigates. This is done whilst considering a single cell scenario where the cell is divided into 3 sectors.

5.1 Framework

Similar to the previous chapter, we consider an ACE scheme which exploits the measurement reports gathered by the UEs but instead of considering a circular cell with an omnidirectional antenna, a 3-sectored cell is used. In this system, UEs measurement reports are tagged with their geographical location information and sent to their serving base station. The serving base station after retrieving the measurement, assigns the UEs to their serving sectors.

The reported geographical coordinates of the UEs and base stations are obtained from positioning techniques such as the observed time difference of arrival (OTDOA) and A-GPS; however as discussed before, these techniques are prone to error which in turn would cause some of the UEs to be tagged to a wrong location.

In this chapter, give a reported UE position, ***o***, with coordinates ***(c, d)***, we assume that the actual location of the UE is within a circular disc with radius ***r***, as shown in FIGURE 3.1(a). Also, we

assume the base station positioning errors can be resolved such that its displacement from its reported position, $\boldsymbol{e}$, is known, as illustrated in FIGURE 4.1. However, this time the circular cell has been divided into three sectors instead of having one big cell for all the UEs, as in FIGURE 5.1.

For analytical tractability, we consider a single cell deployment scenario where RSS measurement reports are gathered by the UE. The signal propagation model we employ for obtaining the RSS is as shown in (9).

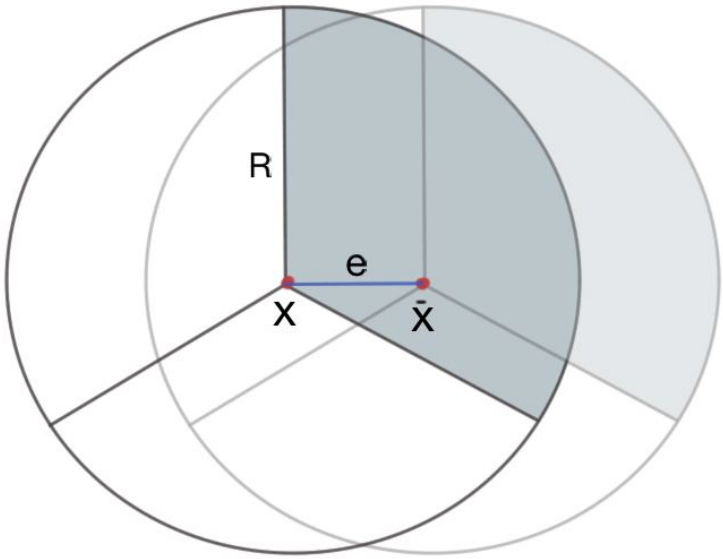

FIGURE 5.1: Circular cell has been divided into three sectors, it has a reported position at X with an actual location $\overline{X}$, which is displaced from X by e.

The probability that the reported RSRP (in dB) at a distance $\boldsymbol{p}$ from the base station will exceed the threshold γ, i.e., $\mathbb{P}\boldsymbol{r}[\boldsymbol{P_r}(\boldsymbol{p}) \geq \boldsymbol{\gamma}]$ as shown in (18), when there are no error in UE and base station location information. In the same way, the cell coverage probability of the ACE scheme without error in location information is shown in (19).

In addition to the UE and base stations position error (considered in chapter 3 and 4), we consider here the scenario where the antenna cell is not omnidirectional and we're having sectored cell.

The measurement reports stored in the TCE are also tagged with a wrong base station position, thus resulting in the generation of a wrong coverage map. In order to estimate the actual coverage probability of the ACE scheme over the area $\mathcal{A}$ (one sector of the circular area) centred at the reported base station position X, we estimate the fraction of the measurement reports that will still be in coverage based on the actual base station position $\bar{X}$.

5.2 Cell Coverage Probability with ACE

In this section, the modified expressions for the actual coverage probability from the ACE scheme is investigated. This is done whilst considering the antenna patterns for a 3-sectored cell with UE and base station errors in the geographical location information.

As we're considering a sectored cell, we need to make use of antenna pattern to modify the expressions we had for the ACE coverage probability and see how the results are affected when there are UE and base station positioning errors.

In order to make use of the antenna pattern parameters, we need to find the antenna azimuth and the tilt. The azimuth, $\varphi(i,k)$, is the angle between antenna main lobe centre and line connecting sector '$\boldsymbol{i}$' and UE '$\boldsymbol{k}$' in radians in horizontal plane whilst the tilt, $\theta(i,k)$, is the angle between antenna main lobe centre and line connecting sector '$\boldsymbol{i}$' and UE '$\boldsymbol{k}$' in radians in vertical plane. The azimuth and tilt angles can be found using (35) and (36) respectively and are shown in FIGURE 5.2 and FIGURE 5.3.

$$\varphi(i,k) = \gamma(i,k) - \xi(i) \tag{35}$$

where ξ is the antenna bearing at sector '$\boldsymbol{i}$' in radians and $\gamma(i,k)$ is the mobile bearing which can be found using atan2 of the UE and BS separation x-axis and y-axis.

$$\theta(i,k) = \omega(i,k) - \zeta(i) \tag{36}$$

where $\omega(i,k)$ is the antenna mobile line of sight angle in radians and ζ is the corrected down tilt angle at sector '$\boldsymbol{i}$' in radians.

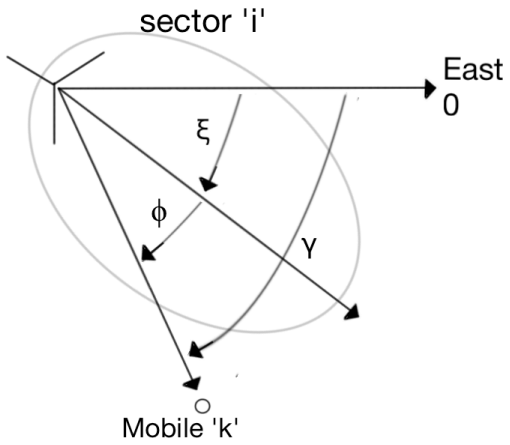

FIGURE 5.2: Mobile bearing orientation diagram - azimuth.

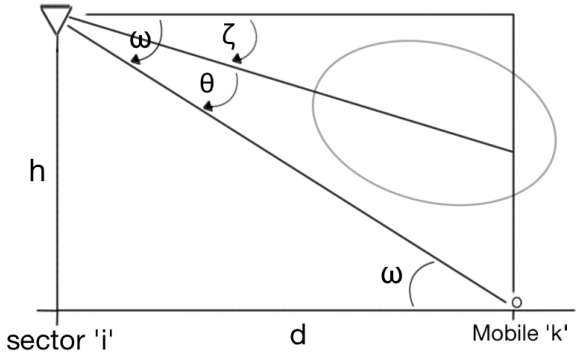

FIGURE 5.3: Mobile bearing orientation diagram - tilt.

For 3-sectored cell sites with fixed antenna patterns, $\varphi(i,k)$ in (35) can be used to find the horizontal antenna pattern $A_H(\varphi)$ as show in (37).

$$A_H(\varphi) = -\min\left[12\left(\frac{\varphi}{\varphi_{3dB}}\right)^2, A_m\right] \quad (37)$$

where A_m represents the maximum front to back ratio in dB and φ_{3dB} represents the horizontal half power bandwidth (az 3dB) in radians.

It can be noted that the horizontal antenna pattern is zero for omnidirectional antennas, $A_H(\varphi) = 0$ (omnidirectional).

Similarly, for a 3-sectored cell sites with fixed antenna patter, $\theta(i,k)$ in (36) can be used to find the vertical antenna pattern $A_V(\theta)$ as shown in (38).

$$A_V(\theta) = -\min\left[12\left(\frac{\theta - \theta_{etilt}}{\theta_{3dB}}\right)^2, SLA_V\right] \quad (38)$$

where SLA_V represents the side lobe attenuation level, θ_{3dB} represents the vertical half power bandwidth (az 3dB) in radians and θ_{etilt} represents the electric antenna down-tilt.

Making use of the horizontal and the vertical antenna patterns and by combining both ((37) and (38)), a representation of the combined 3D antenna pattern can be shown as in (39).

$$A_H(\varphi,\theta) = -\min\{-[A_H(\varphi) + A_V(\theta)], A_m\} \quad (39)$$

Using (39) and by adding the boresight antenna again, the total antenna gain, G_{ant}, is found. This help to find the area mean power, mx, as shown in (40).

$$mx = p_t + G_{ant} - (10\eta \log_{10} d) \quad (40)$$

where p_t is the transmitted power, η is the path-loss exponent and d is the T-R separation.

An approach for evaluating the coverage is to evaluate the radius R based on the threshold and then find the fraction of the area that will not be covered as the result of the geographical error. Alternatively, the number of points on a circular radius defined based on R with RSS (path-loss, transmit power and antenna gain – which is equal in all directions for omnidirectional antennas) greater than or equal to the threshold , γ, can be evaluated. Both methods should give the same results for the case with omnidirectional antennas and no shadowing. However, for the case with shadowing, the first approach is not applicable and the second approach needs to be used.

For the case where we have sectored antenna and no geographical location errors, the number of UEs with RSS greater than or equal to the threshold is evaluated; this is then normalised. Due to the sectored nature of this part, D > R can be selected where D is the T-R separation.

Then for the case with geographical location errors, the number of UEs that were covered when there were no geographical location errors are used and it's evaluated to see if these UEs will still be covered when we add UE and base station geographical errors.

5.3 Numerical Results and Discussions

In this section, we represent the numerical results to show the impact of errors in the reported geographical location information on the actual coverage estimated by the ACE scheme. We consider measurement reports gathered for a single cell, with parameters specified in **Table III** [83] and we estimate the coverage probability over a circular coverage region of area πR^2 where the cell is divided into three sectors and R is assumed to be 500m.

Table III - List of Parameters

Parameters	Symbol	Value (unit)
Standard Deviation	σ	7,9,12 dB
Path-loss Exponent	η	3.5
Reference Distance	P_0	1m
Path-loss at p_0	$Pl(p_0)$	34.5dB
Power Transmitted	P_t	46dBm
Threshold	γ	-84.5dBm
UE Position Error	r	10-100m
Base Station Position Error	e	20m
Horizontal Half Power Bandwidth	φ_{3dB}	70°
Max Front to Back Ratio	A_m	25db
Vertical Half Power Bandwidth	θ_{3dB}	10°
Side Lobe Attenuation Level	SLA_V	20dB
Electric Antenna Down-tilt	θ_{etilt}	15°
Boresight Antenna Gain	$G_{Boresight}$	14 dbi
Base Station Antenna Height	h_{BS}	32m
UE Antenna Height	h_{UE}	1.5m

For the simulation part, 100,000 UEs are distributed following a uniform distribution over the circular cell region of radius R around the base station and their positions are taken as reported positions.

The actual position of the i^{th} UE with coordinated (c_i, d_i) is generated as $\left(c_i + r\sqrt{u_i}\cos(2\pi v_i), d_i + r\sqrt{u_i}\sin(2\pi v_i)\right)$. This is where u_i and v_i are pseudo random, pseudo independent numbers uniformly distributed in [0,1].

For the part with base station position error, the actual coordinates of the base station are obtained using the error e; such that if the reported coordinates were (x, y), the actual coordinates would be obtained as ($x+e$, y).

The RSRP at the actual generated UE position $P_r(\bar{p})$, is estimated according to (9) based on the distance between the actual base station and UE positions; where for the path-loss only channel model, Φ =1.

The cell coverage probability from the ACE scheme is then evaluated as the percentage of UE with $P_r(\bar{p}) \geq \gamma$.

In FIGURE 5.4, we show and compare the coverage probability expression of the ACE scheme for both cases of having only error in the UE geographical location information, and when the base station geographical location information error is added in addition to the error in the UE geographical location information. This is done by using firstly the horizontal antenna pattern and the by using the combined 3D antenna pattern. It can also be noted that the base station position error has been fixed to 20m.

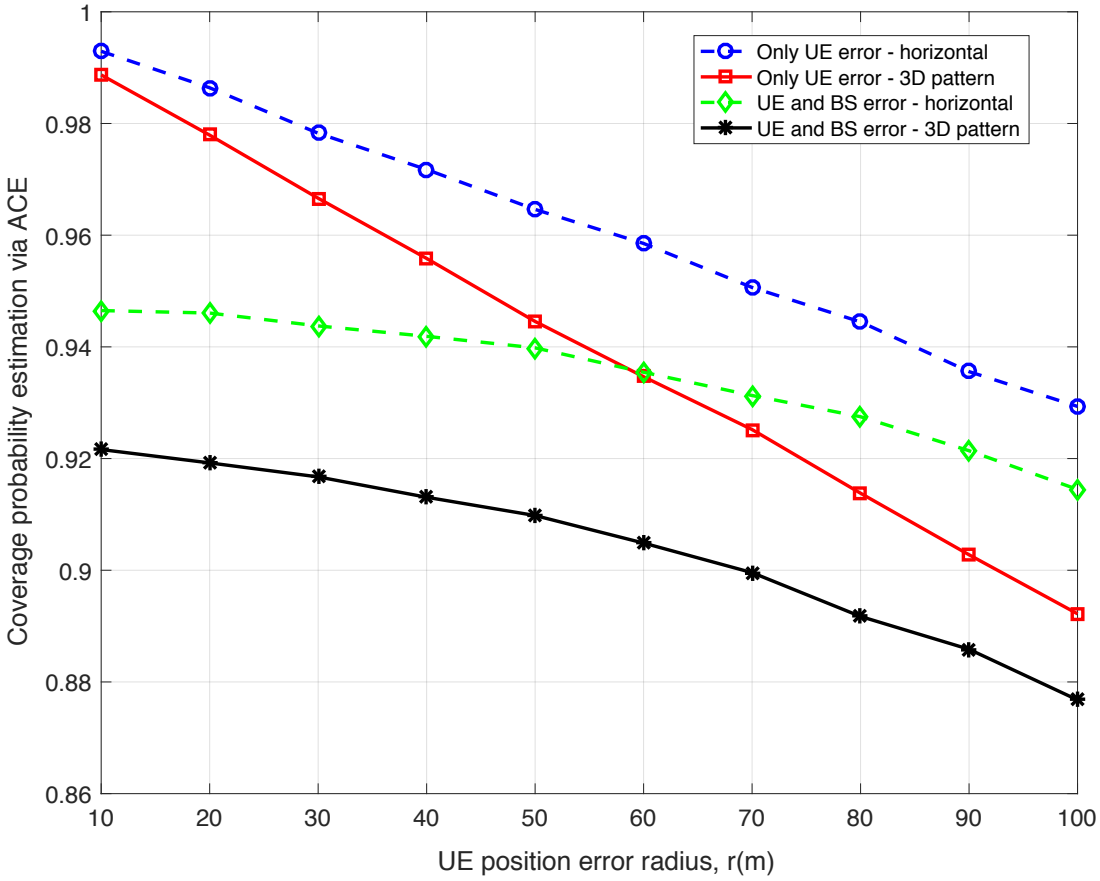

FIGURE 5.4: Coverage probability estimation via ACE, with e=20.

The results in FIGURE 5.4 shows that the error in the cell coverage probability as measured by the ACE scheme increases as the UE position error increases. Also, having base station geographical location information error further degrades the performance of the ACE scheme. It can also be seen that the coverage probability estimation results gathered via using the combined 3D antenna pattern are much less than when we use only the horizontal antenna pattern, the effects of it can be seen more when the base station geographical location information is also included.

In FIGURE 5.5, we show the percentage of the UEs assigned to the wrong sectors due to the errors in the UE and base station geographical location information. Firstly, this is done for the case where we only have UE geographical location information error and then for when the error in the base station geographical location information is added in addition to the UE positioning error.

The results in FIGURE 5.5 shows that the percentage of UEs assigned to the wrong sector increases as the UE position error, r, increases. Furthermore, the percentage of the UE's assigned to the wrong sector are much more when base station positioning error is added. It can also be seen that the difference between the percentage of the UEs assigned to the wrong sectors (both lines on the figure) when UE position error is smaller is much more than when the UE position error it's at its highest.

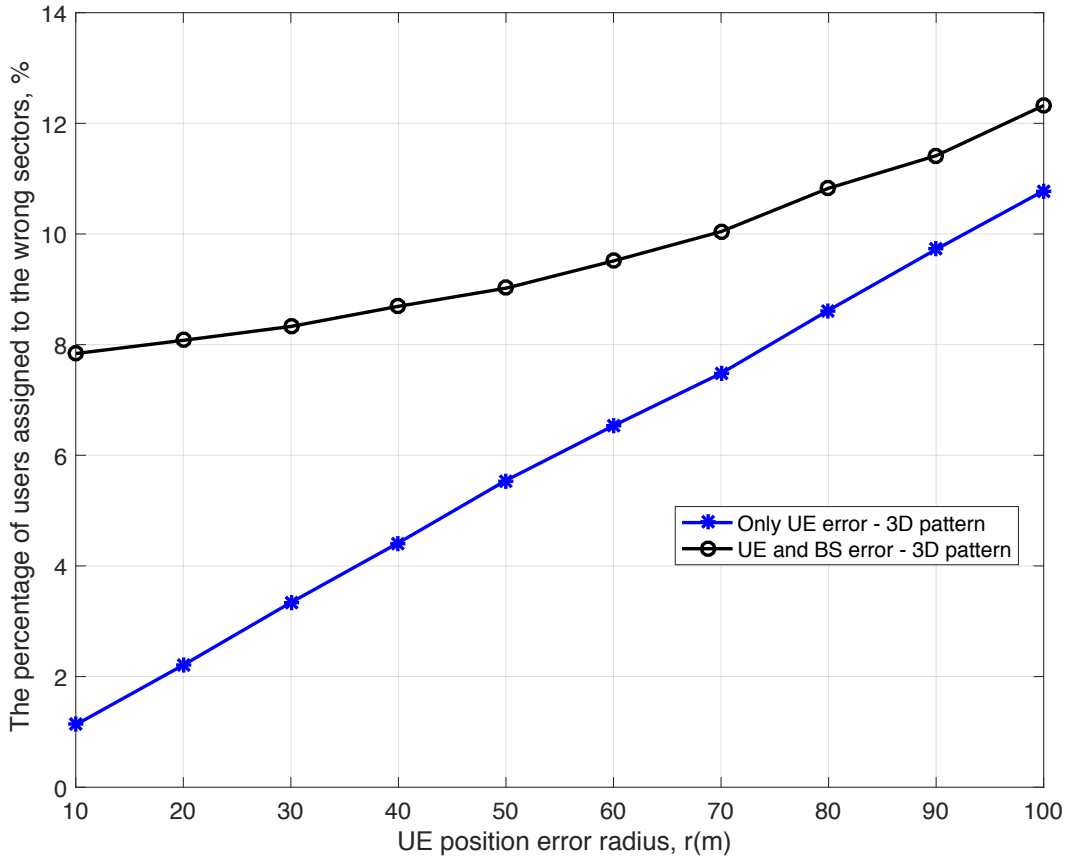

FIGURE 5.5: The percentage of the users assigned to the wrong sectors due to the UE and base station geographical location information errors.

Summary

In this chapter, the effect of error in the user and base station geographical location information on the cell coverage estimation is investigated, this is done whilst considering a three-sectored cell. An ACE scheme is introduced that exploits the measurement reports gathered by the UEs. The error in coverage estimation due to such autonomous scheme is evaluated and the effect of using a three-sectored cell instead of an omnidirectional antenna is investigated.

CHAPTER 6

6 Conclusions and Future Work

This chapter outlines the main technical contributions of this thesis and proposes future research directions as an extension to the work presented here.

6.1 Summary of Insights and Conclusions

We have investigated the impact of inaccurate user equipment (UE) and base station geographical location information on the coverage estimated through a minimisation of drive test (MDT) based autonomous coverage estimation (ACE) scheme.

We have derived the expression of the actual cell coverage probability that can be obtained from such scheme while considering: errors in UE geographical location information and; errors in both UE and base station geographical location information. This had been done for path-loss only channel model in addition to when the shadowing is also considered.

The accuracy of the derived expressions has been shown through numerical results for a range of UE and base station positioning errors. The proposed geographical location information error modified coverage probability estimation expressions tightly match the simulation approach.

We showed that the coverage probability is decreased with the geographical location information error radius in both the shadowing and non-shadowing cases. The reliability of the shadowing case was shown to be approximately equal to 1 when the UE is positioned close to the cell centre, with a steady depreciation as the UE moves away from the cell centre.

Furthermore, it can be observed that the performance of the ACE scheme becomes more degraded and the percentage error in the coverage estimation via ACE increases as the shadowing standard deviation σ reduces. This implies that the errors in UE and base station position estimations are less severe on the coverage as standard deviation σ increases.

We showed that the performance of the ACE scheme will be suboptimal as long as there are errors in the reported geographical location information. Hence, to utilise such ACE scheme, appropriate correction factors that can be calculated using the proposed model must be used.

It's important to note that in this work, RSRP based ACE using MDT measurement report has been presented. Since interference is a key limiting factor in cellular communication, SINR based ACE, which exploits RSRQ (Reference Signal Received Quality) MDT measurement reports, deserves attention in future study.

Also, we considered a three-sectored cell instead of the omnidirectional cell and investigated the impact of inaccurate UE and base station geographical position estimations on the sectors and how they will cause the UEs to be assigned to the wrong sectors.

6.2 Future Work

This section proposes future research guidelines as an extension to the work presented in this thesis.

6.2.1 Antenna Tilt

Antenna tilt is one of the most important system parameters in coverage and capacity optimisation as tilt determines the service coverage boundary and level of inter-cell interference in the system [53].

This is also important in the work proposed in this project as you can determine the coverage of small cells (including the user deployed cells) and at the same time reduce the interference by changing the antenna tilt. So, the next step will be to calculate the antenna tilt angles as a future work. To do so, the macro base station by considering the position of the small cells (including the user deployed cells) and the users, will decide on the coverage of the small cells by telling them to tilt their angles accordingly

6.2.2 Multi Cell

By the increase use of communication networks, the global energy consumption of cellular networks is increasing rapidly. Therefore, greening cellular networks is crucial to reducing the carbon footprint of information and communications technology. This is where multi cell cooperation solution comes into place to improve the energy efficiency of cellular networks [84] [85].

As a future work, the aim is to do all the previous steps but now consider multiple cells (user deployed or fixed operator deployed cells) serving the users and working together to cover all the users (multi cell cooperation).

As shown in [86], green multi cell cooperation (GMC) can be achieved in HetNets facilitated with hybrid energy sources.

6.2.3 Active/Sleep Mode

In order to conserve energy, future radio access networks will activate and deactivate base stations depending on the activity of the users. The UEs that are not in range of a single base station can be reached using cooperative transmissions from base stations. Also when some base stations cooperate, other base stations can be deactivated [87].

This can also be achieved by the traffic-intensity-aware multiple cooperation as discussed in Han et al. [84]. This adapts the network layout of cellular networks according to user demands in order to reduce the number of active base stations.

HetNets composed of various tiers of cells can attain energy savings thanks to the lower operational and transmit power consumptions of small cells. To address the inter-cell interference problem yet achieving network energy conservation, multi cell cooperation facilitating cooperative transmission and sleep mode operation paves a way toward future green HetNets [88].

For the future work, the next step is to include this active/sleep mode scenario for the small cells. If there are not enough users, one (or many) small cells can go to sleep mode in order to reduce the power consumption.

REFERENCES

[1] J. G. Andrews, S. Buzzi, W. Choin, S. V. Hanly, A. Lozano, A. C. K. Soong and J. C. Zhang, "What Will 5G Be?," *IEEE Journal on Selected Areas in Communications,* vol. 32, no. 6, pp. 1065-1082, June 2014.

[2] Cisco, "Cisco Visual Networking Index: Forecast and Methodology, 2016–2021," Cisco White papers, 2017.

[3] A. G. Spilling, A. R. Nix, M. A. Beach and T. J. Harrold, "Self-organisation in future mobile communications," *Electronics & Communication Engineering Journal,* vol. 12, no. 3, pp. 133-147, 2000.

[4] O. G. Aliu, A. Imran, M. A. Imran and B. Evans, "A Survey of self organisation in future cellular networks," *IEEE Communication Surveys and Tutorials,* vol. 15, pp. 336-361, 2013.

[5] NGMN, "NGMN Recommendations on SON and O&M Requirements," Tech. Rep., 2008.

[6] J. L. Van den Berg, R. Litjens, A. Eisenbltter, M. Amirijoo, O. Linnell, C. Blondia, T. Krner, N. Scully, J. Oszmianski and L. C. Schmelz, "Self-Organisation in Future Mobile Communication Networks," in *ICT Mobile Summit*, Sweden, 2008.

[7] R. Combes, Z. Altman and E. Altman, "Self-Organization in Wireless Networks: A Flow-Level Perspective," in *IEEE INFOCOM*, 2012.

[8] Y. Ouyang, Z. Li, L. Su, W. Lu and Z. Lin, "APP-SON: Application characteristics-driven SON to optimize 4G/5G network performance and quality of experience," in *2017 IEEE International Conference on Big Data (Big Data)*, Boston, USA, 2017.

[9] H. Seppo, H. Sanneck and C. Sartori, LTE self-organising networks (SON): network management automation for operational efficiency, John Wiley & Sons, 2012.

[10] A. Mohamed, O. Onireti, M. A. Imran, A. Imran and R. Tafazolli, "Control-Data Separation Architecture for Cellular Radio Access Networks: A Survey and Outlook," *IEEE Communications Surveys & Tutorials,* vol. 18, no. 1, pp. 446-465, 2016.

[11] W. A. Hapsari, A. Umesh, M. Iwamura, M. Tomala, B. Gyula and B. Sebire, "Minimization of drive tests solution in 3GPP," *IEEE Communications Magazine,* vol. 50, no. 6, pp. 28-36, June 2012.

[12] D. Baumann, "Minimization of Drive Tests (MDT) in Mobile Communication Networks," Seminar Future Internet, 2014.

[13] O. Onireti, A. Zoha, J. Moysen, A. Imran, L. Guipponi, M. A. Imran and A. Abu_Dayya, "A Cell Outage Management Framework for Dense Heterogeneous Networks," *IEEE Transactions on Vehicular Technology,* vol. 65, no. 4, pp. 2097-2113, 2016.

[14] A. Zoha, A. Saeed, A. Imran, M. A. Imran and A. Abu-Dayya, "Data-driven analytics for automated cell outage detection in Self-Organizing Networks," in *2015 11th International Conference on the Design of Reliable Communication Networks (DRCN)*, 2015.

[15] T. Kos, M. Grgic and G. Sisul, "Mobile user positioning in GSM/UMTS cellular networks," in *Proceedings ELMAR 2006*, 2006.

[16] 3rd Generation Partnership Project (3GPP), "Evolved Universal Terrestrial Radio Access (E-UTRA); LTE Positioning Protocol (LPP) (Release 11), 3GPP TS 36.355 V11.3.0, 3GPP Std," Technical Speci cation Group Radio Access Network, 2013.

[17] F. Evvenov and F. Marx, "mproving Positioning Capabilities for Indoor Environment with WiFi," in *IST Summit 2005*, 2005.

[18] R. Kaneto, Y. Nakashima and N. Babaguchi, "Real-Time User Position Estimation in Indoor Environments Using Digital Watermarking for Audio Signals," in *2010 20th International Conference on Pattern Recognition*, 2010.

[19] I. Akbari, O. Onireti, M. A. Imran, A. Imran and R. Tafazolli, "Effect of Inaccurate Position Estimation on Self-Organising Coverage Estimation in Cellular Networks," in *20th European Wireless Conference, EW2014*, Barcelona, 2014.

[20] I. Akbari, O. Onireti, A. Imran, M. A. Imran and R. Tafazolli, "Impact of Inaccurate User and Base Station Positioning on Autonomous Coverage Estimation," in *proc IEEE 20th International Workshop on Computer Aided Modelling and Desing of Communication Links and Networks, CAMAD 2015*, 2015.

[21] I. Akbari, O. Onireti, A. Imran, M. A. Imran and R. Tafazolli, "How Reliable is MDT-Based Autonomous Coverage Estimation in the Presence of User and BS Positioning Error?," *IEEE Wireless Communications Letters,* vol. 5, no. 2, pp. 196-199, 2016.

[22] A. Anpalagan, “HetNet Radio Resource Management, Access and Networking,” [Online]. Available: www.ee.ryerson.ca.

[23] H. Klessig, D. Öhmann, A. I. Reppas, H. Hatzikirou, M. Abedi, M. Simsek and G. P. Fettweis, “From Immune Cells to Self-Organizing Ultra-Dense Small Cell Networks,” *IEEE JOURNAL ON SELECTED AREAS IN COMMUNICATIONS,* vol. 34, no. 4, pp. 800-811, April 2016.

[24] Qualcomm Incorporate, “LTE Advanced: Heterogeneous Networks,” 2011.

[25] W. Noh, W. Shin, C. Shin, K. Jang and H.-H. Choi, “Distributed Uplink Intercell Interference Control in Heterogeneous Networks,” in *2012 IEEE Wireless Communications and Networking Conference (WCNC)*, 2012.

[26] Y. S. Soh, T. Q. S. Quek, M. Kountouris and H. Shin, “Energy Efficient Heterogeneous Cellular Networks,” *IEEE Journal on Selected Areas in Communications,* vol. 31, no. 5, pp. 840-850, 2013.

[27] D. Karvounas, P. Vlacheas, A. Georgakopoulos, M. Logothetis, V. Stavroulaki, K. Tsagkaris and P. Demestichas, “Coverage and Capacity Optimisation in Heterogeneous Networks (HetNets): A Green Approach,” in *ISWCS 2013; The Tenth International Symposium on Wireless Communication Systems*, 2013.

[28] H. Ishii, Y. Kishiyama and H. Takahashi, “A novel architecture for LTE-B :C-plane/U-plane split and Phantom Cell concept,” in *IEEE Globcom Workshops*, Anaheim, CA, USA, 2012.

[29] Z. Ghadialy, “The Phantom Cell Concept,” 2013. [Online]. Available: blog.3g4g.co.uk.

[30] S. Mukherjee and H. Ishii, “Energy Efficiency in the Phantom Cell Enhanced Local Area Architecture,” in *2013 IEEE Wireless Communications and Networking Conference (WCNC)*, 2013.

[31] 3GPP, “3GPP LTE Release 12,” 2012.

[32] J. G. Andrews, F. Baccelli and R. K. Ganti, “A Tractable Approach to Coverage and Rate in Cellular Networks,” *IEEE Transactions on Communications,* vol. 59, no. 11, pp. 3122-3134, 2011.

[33] H. Haken, “Self-organization,” Scholar pedia, 2008.

[34] S. Haykin, “Cognitive Radio: Brain-empowered wireless communications,” *IEEE Journal on Selected Areas in Communications,* vol. 23, no. 2, pp. 201-220, 2005.

[35] Nokia Siemens Networ, “Self-organizing networks (SON)”.

[36] I. Poole, “Self-Organising networks, SON,” [Online]. Available: www.radio-electronics.com.

[37] M. Peng, D. Linag, Y. Wei, J. Li and H.-H. Chen, "Self-configuration and self-optimization in LTE-advanced heterogeneous networks," *IEEE Communications Magazine,* vol. 51, no. 5, pp. 36-45, 2013.

[38] H. Zhang, Y. Wang and H. Ji, "Resource Optimization-Based Interference Management for Hybrid Self-Organized Small-Cell Network," *IEEE Transactions on Vehicular Technology,* vol. 65, no. 2, pp. 936-946, 2016.

[39] M. Nohrborg, "Self-organising networks," 3GPP, [Online]. Available: 3GPP.org/technologies.

[40] H. Hu, J. Zhang, X. Zheng, Y. Yang and P. Wu, "Self-configuration and self-optimization for LTE networks," *IEEE Communications Magazine,* vol. 48, no. 2, pp. 94-100, 2010.

[41] 3GPP, "Overview of 3GPP Release 9," September 2014. [Online]. Available: www.3gpp.org.

[42] "LTE SON on Self-Healing," November 2011. [Online]. Available: LTEguide.blogspot.co.uk.

[43] M. Dottling and I. Viering, "Challenges in mobile network operation: Towards self-optimizing networks," in *2009 IEEE International Conference on Acoustics, Speech and Signal Processing*, 2009.

[44] O. N. C. Yilmaz, J. Hämäläinen and S. Hämäläinen, "Self-optimization of remote electrical tilt," in *21st Annual IEEE International Symposium on Personal, Indoor and Mobile Radio Communications*, 2010.

[45] O. N. C. Yilmaz, J. Hämäläinen and S. Hämäläinen, "Self-optimization of Random Access Channel in 3GPP LTE," in *2011 7th International Wireless Communications and Mobile Computing Conference*, 2011.

[46] H. Y. Lateef, A. Imran and A. Abu-dayya, "A Framework for Classification of Self-Organising Network Conflicts and Coordination Algorithms," in *Personal, Indoor and Mobile Radio Communications (PIMRC): Mobile and Wireless Networks*, 2013.

[47] W. Wang, J. Zhang and Q. Zhang, "Transfer Learning Based Diagnosis for Configuration Troubleshooting in Self-Organizing Femtocell Networks," in *2011 IEEE Global Telecommunications Conference - GLOBECOM 2011*, 2011.

[48] F. Parodi, M. Kylvaja, G. Alford, J. Li and J. Paradas, "An automatic procedure for neighbor cell list definition in cellular networks," in *2007 IEEE International Symposium on a World of Wireless, Mobile and Multimedia Networks*, 2007.

[49] 3GPP, "3GPP work items on Self-Organising Networks," June 2014. [Online]. Available: www.3gpp.org.

[50] I. Poole, “SON Self Configuration,” [Online]. Available: http://www.radio-electronics.com/.

[51] 3GPP, “Telecommunication management; Self-Organising Networks (SON) Policy Network Resource Model (NRM) Integration Reference Point (IRP);Information Service (IS) Release 11, TS 32.522,” September 2011. [Online]. Available: www.3gpp.org.

[52] T. Bandh, R. Roemikat, H. Sanneck and H. Tang, “Policy-based Coordination and Management of SON Functions,” in *12th IFIP/IEEE International Symposium on Integrated Network Management (IM 2011) and Workshops*, 2011.

[53] I. Luketic, D. Simunic and T. Blajic, “Optimization of coverage and capacity of Self-Organizing Network in LTE,” in *2011 Proceedings of the 34th International Convention MIPRO*, 2011.

[54] L. Meyer and J. Syed, “Antenna Technology in the LTE Era,” October 2013. [Online]. Available: www.radio-electronics.com.

[55] D. Jefferies, “Antennas,” [Online]. Available: http://personal.ee.surrey.ac.uk/.

[56] D. W. Kifle, B. Wegmann, I. Viering and A. Klein, “On the potential of traffic driven tilt optimization in LTE-A networks,” in *2013 IEEE 24th Annual International Symposium on Personal, Indoor, and Mobile Radio Communications (PIMRC)*, 2013.

[57] A. Imran, M. A. Imran, A. Ul-Quddus and R. Tafazolli, “Distributed Spectral Efficiency Optimisation at Hotspot Through Self Organisation of BS Tilt,” in *2011 IEEE GLOBECOM Workshops (GC Wkshps)*, 2011.

[58] CISCO, “Antenna Pattern and Their Meanings,” [Online]. Available: www.cisco.com.

[59] M. Rouse, “Azimuth and Elevation,” 2006. [Online]. Available: whatistechtarget.com.

[60] Mobile Mark, “Antenna Technology defined,” [Online]. Available: www.mobilemark.com/engineering/antenna-theory-simplified.html.

[61] “Satellite Antenna Bearing Calculation,” [Online]. Available: giangrandi.ch.

[62] S. Hamalainen , H. Sanneck and C. Sartori, LTE Self-Organizing Networks (SON): Network Management Automation for Operational Efficiency, Wiley, 2011.

[63] T. Bandh, H. Sanneck and R. Romeikat, “An Experimental System for SON Function Coordination,” in *Vehicular Technology Conference (VTC Spring)*, 2011.

[64] L. C. Schmelz, M. Amirijoo, A. Eisenblaetter, R. Litjens, M. Neuland and J. Turk, “A Coordination Framework for Self-Organisation in L TE Networks,” in *12th IFIP/IEEE International Symposium on Integrated Network Management (IM 2011) and Workshops*, 2011.

[65] H. Y. Lateef, A. Imran, M. A. Imran, L. Giupponi and M. Dohler, "LTE-advanced self-organizing network conflicts and coordination algorithms," *IEEE Wireless Communications,* vol. 22, no. 3, pp. 108-117, 2015.

[66] NGMN, "A Deliverable by the NGMN alliance: NGMN top OPE recommendations," 2010.

[67] Technical Specification group Radio Access Networks, "Study on Minimisation of drive tests in next generation networks (Release 9)," 3GPP, 2009.

[68] J. Johansson, W. A. Hapsari, S. Kelley and G. Bodog, "Minimization of drive tests in 3GPP release 11," *IEEE Communications Magazine,* vol. 50, no. 11, November 2012.

[69] P.-C. Lin, "Minimization of Drive Tests Using Measurement Reports From User Equipment," in *Consumer Electronics (GCCE), 2014 IEEE 3rd Global Conference on*, Tokyo, Japan, 2014.

[70] T. Hiltunen, R. U. Mondal, J. Turkka and T. Ristaniemi, "Generic Architecture for Minimizing Drive Tests in Heterogeneous Networks," in *Vehicular Technology Conference (VTC Fall), 2015 IEEE 82nd*, Boston, MA, USA, 2015.

[71] F. Chernogorov and J. Puttonen, "User Satisfaction Classification for Minimization of Drive Tests QoS Verification," in *Personal Indoor and Mobile Radio Communications (PIMRC), 2013 IEEE 24th International Symposium on*, London, UK, 2013.

[72] F. Evennov and F. Marx, "Improving Positioning Capabilities for Indoor Environment with WIFI," in *IST Summit*, 2005.

[73] J. Hightower, G. Borriello and R. Want, "SPOTON: an Indoor 3D Location Sensing Technology Based on RF Signal Strength," Uni. Washington CSE Tech Report, 2000.

[74] N. Priyantha, A. Chakraborty and H. Blackrishnan, "The Cricket Location Support System," in *MOBICOM*, 2000.

[75] R. Kaneto, Y. Nakashima and N. Babaguchi, "Real-Time User Position Estimation in Indoor Environments Using Digital Watermarking for Audio Signals," in *2010 20th International Conference on Pattern Recognition*, 2010.

[76] E. C. L. Chan, G. Baciu and S. C. Mak, "Wireless Tracking Analysis in Location Fingerprinting," in *2008 IEEE International Conference on Wireless and Mobile Computing, Networking and Communications*, 2008.

[77] C. Takenga and K. Kyamakya, "A Low Cost Fingerprint Positioning System in Cellular Networks," in *2007 Second International Conference on Communications and Networking in China*, 2007.

[78] R. Mondal, J. Turkka and T. Ristaniemi, "An Efficient Grid-Based RF Fingerprint Positioning Algorithm for User Location Estimation in Heterogeneous Small Cell

Networks," in *International Conference on Localization and GNSS 2014 (ICL-GNSS 2014)*, 2014.

[79] K. Tsuji and E. Kamioka, "Estimation of Users Position and Behaviour Based on Measurements of Sensor Information," in *2009 International Symposium on Autonomous Decentralized Systems*, 2009.

[80] S. A. Hoseinitabatabaei, A. Gluhak and R. Tafazolli, "Towards a Position and Orientation Independent Approach for Pervasive Observation of User Direction with Mobile Phones," *Pervasive and Mobile Computing Journal,* 2014.

[81] W. C. Jakes, Microwave Mobile Communications, 2nd ed., IEEE Press, 1994.

[82] T. S. Rappaport, Wireless Communications - Principles and Practice, 2nd ed., Prentice Hall, 2002.

[83] 3GPP, "Technical Specification Group Radio Access Network; Further Advancements for E-UTRA Physical Layer Aspects (Release 9)," 2010.

[84] S. Han, C. Yang, G. Wang and M. Lei, "On the energy efficiency of base station sleeping with multicell cooperative transmission," in *2011 IEEE 22nd International Symposium on Personal, Indoor and Mobile Radio Communications*, 2011.

[85] X. Wang, F.-C. Zheng , P. Zhu and X. You, "Energy-Efficient Resource Allocation in Coordinated Downlink Multicell OFDMA Systems," *IEEE Transactions on Vehicular Technology,* vol. 65, no. 3, pp. 1395-1408, 2016.

[86] Y.-H. Chiang and W. Liao, "Green Multicell Cooperation in Heterogeneous Networks With Hybrid Energy Sources," *IEEE Transactions on Wireless Communications,* vol. 15, no. 12, pp. 7911-7925, Dec 2016.

[87] M. Herlich and H. Karl, "Energy-Efficient Assignment of User Equipment to Cooperative Base Stations," in *ISWCS 2013; The Tenth International Symposium on Wireless Communication Systems*, 2013.

[88] Y.-H. Chiang and W. Liao, "ENCORE: An energy-aware multicell cooperation in heterogeneous networks with content caching," in *IEEE INFOCOM 2016 - The 35th Annual IEEE International Conference on Computer Communications*, San Francisco, USA, 2016.

[89] J. Hightower, G. Boriello and R. Want, "SPOTON: An Indoor 3D location Sensing Technology Based on RF Signal Strength," in Uni. Washington CSE Tech Report, 2000.